haematologica
Journal of the Ferrata Storti Foundation

# Platelets-driven monocyte activation promotes hypoxic thromboinflammation through the HIF-1α-NLRP3-EGR-1 axis

*by Shankar Chanchal, Kashika Singh, Raishal Safdar, Syed Mohd, Tashi Thinlas, Sayeed Ahmad, Tathagata Chatterjee and Mohammad Zahid Ashraf*

*Received: January 7, 2025.*
*Accepted: October 1, 2025.*

*Citation: Shankar Chanchal, Kashika Singh, Raishal Safdar, Syed Mohd, Tashi Thinlas, Sayeed Ahmad, Tathagata Chatterjee and Mohammad Zahid Ashraf. Platelets-driven monocyte activation promotes hypoxic thromboinflammation through the HIF-1α-NLRP3-EGR-1 axis.*
*Haematologica. 2025 Oct 9. doi: 10.3324/haematol.2025.287317 [Epub ahead of print]*

# Platelets-driven monocyte activation promotes hypoxic thromboinflammation through the HIF-1α-NLRP3-EGR-1 axis

Shankar Chanchal[1], Kashika Singh[1], Raishal Safdar[1], Syed Mohd[1], Tashi Thinlas[2], Sayeed Ahmad[3], Tathagata Chatterjee[4], Mohammad Zahid Ashraf[1*]

[1]Department of Biotechnology, Faculty of Life Sciences, Jamia Millia Islamia, New Delhi, India
[2]Department of Medicine, Sonam Norboo Memorial Hospital, Leh, Ladakh
[3]Department of Pharmacognosy and Phytochemistry, Jamia Hamdard, New Delhi
[4]Department of Hematology, ESIC Medical College, Faridabad, Haryana

**Running title:** Inflammation induced coagulation under hypoxia

***Correspondence:**

Mohammad Zahid Ashraf, Ph.D.
Professor, Department of Biotechnology
Jamia Millia Islamia
New Delhi - 110025, INDIA
Mob: +91 9871426706
Email: zashraf@jmi.ac.in, mohammadzashraf@gmail.com

**Keywords:** Hypoxia, NLRP3 inflammasome, Venous Thromboembolism, Thromboinflammation, EGR-1, Tissue Factor, Immune cells, HIF-1α

## ACKNOWLEDGEMENTS

We thank Central Drug Research Institute (CDRI), Lucknow, India, and Institute of Genomics and Integrative Biology (IGIB), Delhi, India for the kind gift with the cell line. We are grateful to the Department of Medicine, Sonam Norboo Memorial Hospital, Leh, Ladakh and the

Department of Hematology, ESIC Medical College, Faridabad, Haryan, India for the human sample study.

**Funding**

The Department of Biotechnology (DBT), Govt of India, and the Scheme for Promotion of Academic and Research Collaboration (MHRD-SPARC) has supported this research project. S. Chanchal is recipient of Senior Research fellowship from The Council of Scientific and Industrial Research (HRDG-CSIR).

## AUTHOR CONTRIBUTIONS

S. Chanchal and M. Z. Ashraf designed and wrote the manuscript as per the study. S. Chanchal performed the experiments and interpreted the data. K. Singh, R. Safdar and S. Ahmad helped in experiments and data interpretation. S. Mohd and T. Thinlas collected blood of human samples, and all authors edited and finally approved the latest version of the manuscript.

## Data sharing and availability

The data were generated at Jamia Millia Islamia, Delhi, India. The data supporting the findings and details methods are available from the corresponding author on request.

## DECLARATION OF CONFLICT-OF-INTEREST

All the authors declared no conflicts of interest.

**Abstract (250)**

Hypoxia exacerbates thromboembolism and sterile inflammation through NLRP3 inflammasome, which is directly activated by HIF-1α that plays a pivotal role in potentiating deep vein thrombosis (DVT). One of the clinical manifestations of thromboinflammation is DVT, characterized by formation and propagation of clot in the lower extremity of the body. The underlying inflammatory milieu promotes immune cell recruitment and platelet hyperactivation, further promoting a prothrombotic state. However, the intricate relationship between hypoxia, thromboembolism, and sterile inflammation is not fully understood. To address this knowledge gap, we integrated *in vitro cell lines, ex vivo* human primary blood mononuclear cells (hPBMCs), *in vivo* animal models, and human patient-based studies to uncover the role of cellular interactions in driving hypoxia-induced thrombosis. We identified the early mechanistic insights and subsequently tested the translational potential in human samples who developed DVT at high altitudes (altitude >11,000 feet). Our investigation revealed that hypoxia increased monocyte adhesion to endothelial surface, mediated through CD11a/CD18 (β2 integrin) and F11R (Junctional adhesion molecule-1; JAM-1). We identified the significance of the HIF-1α-NLRP3-Egr1-TF/FVII axis in inflammation-induced coagulation under sterile conditions operating through NLRP3 elevating Egr-1, which subsequently augments tissue factor. This axis increases platelet hyperactivation and platelets' association amplifying thromboinflammation. Human patients who developed high altitude thrombosis revealed enhanced HIF-1α, NLRP3, Egr1, and TF/FVII levels, confirming clinical relevance. Finally, abrogating these molecules either with pharmacological inhibitors or siRNAs have demonstrated a potential to reverse these pathophysiological processes. These finding identify the HIF-1α-NLRP3-Egr1-TF/FVII axis as a potential therapeutic target for mitigating hypoxia induced thromboinflammation.

**Introduction**

Venous thromboembolism (VTE) is one of the most significant contributors of cardiovascular morbidity and mortality worldwide, closely following stroke and myocardial infarction.[1-4] This underscores the necessity of effective population-level strategies. The initiation of thromboembolism is a multifactorial process involving complex events complying with Virchow's Triad.[5] We previously reported that sterile inflammation plays a critical role in the

pathogenesis of VTE under hypoxic conditions, demonstrating the activation of the nucleotide-binding domain, leucine-rich-containing family, pyrin domain-containing-3 (NLRP3) inflammasome in hypoxia and its direct regulation by HIF-1α.[6]

Hypoxia, characterized by low oxygen availability at both systemic and localized levels caused by blood flow restriction or stasis, contributes significantly to thrombus formation.[7] Unfavorable environmental factors, such as hypobaric hypoxia and low temperature, also aggravates prothrombotic phenotype at high to extreme altitudes (4921 to 11,483 feet).[8] Multiple research groups have shown a link between hypoxia and inflammatory responses, involving different cell types such as endothelial cells, lymphocytes, monocytes, and platelet activation.[9-11] Furthermore, hypoxic exposure results in activation of endothelial cells and recruitment of different immune cells, such as monocytes/macrophages, neutrophils, and lymphocytes, to the venous wall, resulting in blood clot formation[11]. Platelets directly participate in this process, resulting in amplification of thrombi.[12-13] Beyond their primary role in adhesion and aggregation, platelets contribute to thrombosis through several other mechanisms, such as triggering coagulation, generating platelet-leukocyte aggregation, enhancing extracellular traps (NETs) formation from neutrophils, activating NLRP3 inflammasome that results in the release of IL-1β and IL-18.[14-15]

While the activation of the NLRP3 inflammasome is a key upstream event, the specific transcriptional regulators that translate this inflammatory signal into a pro-coagulant state during hypoxia are not well defined. In the last two decades many groups have shown Early Growth Response-1 (Egr-1) plays a crucial role in inflammation and coagulation.[16-17] Egr-1 is a prototypic member of egr family of zinc finger transcription factor which is stimulated by various stimuli in different cell types. Pawlinski *et al.*, have showed the sustained expression of inflammatory mediators and tissue factor in endotoxemia model.[16] Wu et al., have demonstrated that thrombin stimulates Egr-1 expression in endothelial cells via a MAPK-dependent mechanisms.[17]

However, a direct mechanistic link between hypoxia-driven HIF-1α-NLRP3 axis and the transcriptional activation of pro-coagulant factors remain poorly defined. In this study, we sought to bridge this gap by investigating the downstream effectors of inflammasome activation in thromboinflammation. Using in vitro cell lines, hPBMCs, a murine model of hypoxia-induced thrombosis, and DVT patients exposed to high altitude, we demonstrate that the HIF−1α−NLRP3 axis promotes thrombosis by upregulating Egr−1 and its target, Tissue Factor (TF). This study

also highlights that this pathway enhances monocyte recruitment and is amplified by hyperreactive platelets, which further stimulate NLRP3 activation in monocytes. Our findings establish the HIF−1α−NLRP3−Egr−1−TF axis as a central driver of hypoxia-induced thrombosis, offering new targets for therapeutic intervention.

## Methods

### Cell lines, primary human cells isolation and culture conditions

THP-1, human leukemia monocytic cell line, and K-562, human myelogenous leukemia cell line, were obtained from the National Centre for Cell Science (NCCS) Pune, India. Human umbilical vein cell lines (Ea. hy926 and HUVECs) were a kind gift from Central Drug Research Institute (CDRI), Lucknow, India, and Institute of Genomics and Integrative Biology (IGIB), Delhi, India respectively.

### In vitro experimental treatments

THP-1 and K-562 were differentiated using Phorbol 12-myristate 13-acetate (PMA) (see *online supplementary section for protocol*). The cells were treated with 1% Oxygen ($O_2$) for hypoxic condition for 8h, Dimethyloxalylglycine (DMOG-1000μM) for HIF-1α activator for 12h. For inhibition studies, cells were treated with 3,3'-Diindolylmethane (DIM-10μM) for HIF-1α inhibitor, after DMOG stimulation; pre-treated with for 4h with MCC950-10μM for NLRP3 inhibitor and SML0499-10μM for inhibition of catalytic activity of Caspase-1, prior to DMOG stimulation. Adenosine diphosphate (ADP-10μM) was used for the activation of platelets, which was washed with fresh media before using for experiments.

### Animals and Treatment

All the experiments were performed according to the guidelines set forth by the Committee for Control and Supervision of Experiments on Animals, Government of India. The male Wistar rats of 220-250g weight kept and cared in a typical standard laboratory setting for the investigation. The animals were divided into seven groups, (A) NA/Control, (B) Heparin, (C) $FeCl_3$ induced, (D) DMOG, (E) DMOG+DIM, (F) MCC950+DMOG and, (G) SML0499+DMOG. All the chemicals were injected intravenously through the tail vein.

**Human Studies**

Human studies were conducted in accordance with the ethical standards of Indian Council of Medical Research. The DVT patients (n=10) at high altitude in Leh Ladakh (altitude >11,483 feet) who reported to the only immediate care facility, Sonam Nurboo Memorial (SNM) Hospital, the district hospital of Leh, Ladakh, India (altitude ~ 11500 ft), and the low lander patients with VTE and associated complications (n=5) at ESIC Medical College, Faridabad, India were included in the study.

The highlander and lowlander patients were examined by physicians at SNM Hospital or ESIC medical college respectively, and blood samples were collected via venipuncture as soon as possible following confirmation of diagnosis, which was performed using ultrasound imaging, were approached and informed consent was obtained according to the Declaration of Helsinki. The control group comprised a comparable number of healthy volunteers, matched for ethnicity and duration of stay at high altitude, who did not develop any form of thrombosis during the same period, while low lander healthy controls were healthy individuals residing in plains. Individuals with pre-existing systemic diseases, malignancies, sickle cell anemia, paroxysmal nocturnal hemoglobinuria, lupus anticoagulant, or those who had undergone prior surgery were excluded from the study. Peripheral blood mononuclear cells collected from healthy volunteers were isolated by density gradient centrifugation.

**Statistical analysis**

All the statistical analysis was performed using GraphPad Prism (v.8), R studio and SPSS. Unless specified otherwise, all results included were represented as mean ± S.E.M. One-way ANOVA with the Tukey’s multiple comparison post hoc test was applied to compare data across several groups, the unpaired, two-tailed Student's t-test was employed to compare two groups of independent samples, linear regression and Pearson Correlation analysis was applied. The statistical analysis for all the data was done and represented as p-values.

## Results

### HIF-1α-NLRP3 inflammasome axis in monocytes induces its adhesion to endothelial cells

The monocyte adhesion to endothelium depends on their adhesion molecules, this is a crucial step in regulating vascular inflammation.[19] The direct association of HIF-1α-NLRP3 on leukocyte function in thrombosis remains unclear. To assess the impact of the HIF-1α-NLRP3-inflammasome axis on monocyte adherence to vascular endothelium, we performed monocytes-endothelial cell adhesion assay. Endothelial cells (Ea. hy926 or HUVECs) were pre-activated with 1% oxygen for 8h to create an adhesive surface for monocytes. THP-1 and hPBMCs were treated with 1% oxygen or DMOG in the presence or absence of the inhibitors DIM, MCC950, and SML0499. Compared to the control (activated endothelial cells with monocytes with no additions or exposures), exposing monocytes to either hypoxia or HIF-1α activator (DMOG) exhibited a similar (8-9-fold) increase in the total number of monocytes adhered to the surface of endothelial cells. This effect was significantly reversed when monocytes were treated with inhibitors of HIF-1α (DIM), NLRP3 (MCC950), or Caspase-1 (SML0499) confirming that the adhesion was dependent on this specific pathway (Figure 1A, and S1).

We next examined the effect of ADP-induced activated platelets on monocytes adhesion to hypoxia-activated endothelial cells. In the presence of ADP-induced platelets, monocyte adhesion increased significantly under various conditions: 5.7-fold increase was observed in monocytes without hypoxia treatment, 18.3-fold increase in monocytes exposed to hypoxia, and 15-fold increase in DMOG-treated monocytes. These fold changes are relative to normoxic monocytes adhered to hypoxia-activated endothelial cells, highlighting the enhanced adhesive response induced by activated platelets. DIM, MCC950, and SML0499 showed comparable decrease in the monocyte adhesion to hypoxic endothelial cells compared to DMOG (Figure 1B).

To understand the molecular basis, we examined the expression of key adhesion molecules- β2 integrin (CD11a/18) and junctional adhesion molecule-1 (JAM-1). A significant increase in the expression of CD11a/18 ($p=1.09E-12$) and F11R ($p=6.9E-13$) was observed under hypoxic conditions and in the presence of DMOG. This increased expression was significantly reduced by the pharmacological inhibition of HIF-1α, NLRP3, and Caspase-1 activity, suggesting that monocyte adhesion to activated endothelial cells under hypoxia may be mediated through these

molecules. Further validation is needed to confirm this mechanism (Figure 1C and D). Figure 1E illustrates monocyte adhesion to endothelial cells under various experimental conditions.

CD11a/18 (β2 integrin) is expressed by monocytes and other leukocytes, but not by endothelial cells (ECs).[20] Endothelial cells, monocytes, and platelets including others express F11R.[21] We examined the expression of F11R separately in monocytes and endothelial cells. The results demonstrated that the expression of F11R independently under hypoxia and DMOG, was modestly upregulated in monocytes (~1.8 fold) and in ECs (~1.9-fold) under hypoxia (Figure S2). In contrast, co-culturing these cells resulted in amplification of F11R expression to a level 3.5-fold higher than in separate cultures (Figure 1D). The increased expression of F11R in the co-culture is due to the interaction between monocytes and ECs not by ECs only. This data collectively suggests that the HIF-1α-NLRP3 axis enhances monocyte adhesion to endothelial cells, potentially through the upregulation of β2 integrin and F11R expression.

Furthermore, we observed the expression of adhesion molecules in ECs and found increased expression of I-CAM, V-CAM, E-selectin and P-selectin under hypoxia, DMOG which was suppressed in DIM, MCC950 and SML0499 signifying the importance of endothelial dysfunction/activation for the recruitment of immune cells and the progression of thrombosis through HIF-1α-NLRP3 axis (Figure S3).

**Status of hypoxia and its response pathway in manifesting NLRP3 inflammasome activation leading to increased expression of Egr-1 in monocytes through HIF-1α-NLRP3 axis**

The involvement of the HIF-1α-NLRP3 axis in potentiating thrombosis engenders us to inspect the functional engrossment of hypoxia response pathways. The expression of HIF-1α protein (Figure 2A), and its targeted transcripts, VEGF-A (vascular endothelial growth factor-A), and EPO (erythropoietin) (Figure S4), were significantly increased under hypoxia and DMOG. The presence of a pharmacological inhibitor of HIF-1α, NLRP3, and Caspase-1 resulted in reduced accumulation and transcriptional activity of VEGF-A and EPO in monocytes (Figure S4).

Further, we investigated the association between hypoxia, HIF-1α and NLRP3 inflammasome activation in monocytes. We observed a significant increase in protein levels of NLRP3, and IL-1β (Figure 2B and 2C) and mRNA transcripts of NLRP3, Caspase-1 and IL-1β. Apart from this,

caspase-1 catalytic activity and IL-1β release were significantly increased under hypoxia and DMOG (Figure 2B-C, S4). Their expression was downregulated by DIM, MCC950, and SML0499, indicating the activation of NLRP3 under hypoxia in monocytes/macrophages.

Following hypoxia pathway modulation and, NLRP3 inflammasome activation, we observed a significant increase in both mRNA and protein levels of Egr-1 under hypoxia (p=2.6E-11, p=8.4E-9) and DMOG (p=9.0E-13, p=2.7E-10). This upregulation was completely dependent on the integrity of this axis as Egr-1 levels is decreased significantly under the pharmacological inhibition of HIF-1α (DIM: p=5.0E-10, p=1.2E-7), NLRP3 (MCC950: p=9.1E-13, p=4.5E-10), and the catalytic activity of Caspase-1 (SML0499: p=9.0E-13, p=1.7E-11) (Figure 2D, S4). In hPBMCs, Egr-1 mRNA expression was upregulated in hypoxia and DMOG which was suppressed by inhibiting HIF-1α, NLRP3, and catalytic activity of caspase-1 indicating the regulation of Egr-1 under hypoxia is due to HIF-1α-NLRP3 axis. (Figure S4A).

To determine if HIF-1α regulates Egr-1 directly, we performed Chromatin Immunoprecipitation (ChIP) assays. The binding of HIF-1α to the promoter region of Egr-1 gene was analyzed through ChIP assays under different experimental conditions (Figure 2E). The enrichment of Egr-1 promoter region in ChIP assays demonstrated increased binding of HIF-1α to the promoter in hypoxia and DMOG-treated samples, while this binding was substantially reduced in the presence of DIM, MCC950, and SML0499 (Figure S4).

To further investigate the specific interaction between HIF-1α and Egr-1 promoter, we identified that HIF-1α binds to the hypoxia response element (HRE) region within Egr-1 promoter. HIF-1α binds to the HRE sequence 5'-TCACGTCA-3', spanning nucleotides -869 to -862. Additionally, three HRE binding sites for HIF-1α were identified in the Egr-1 promoter at nucleotide positions -1302 to -1295, -1585 to -1578, and -869 to -862 (Figure 2F).

These findings illustrate that HIF-1α directly binds to the HRE regions within the Egr-1 promoter, suggesting that the regulation of Egr-1 expression under these conditions is mediated by HIF-1α binding.

**Role of HIF-1α-NLRP3 inflammasome axis in the coagulation cascade potentiating thrombosis in monocytes**

To establish the functional role of the HIF-1α-NLRP3 inflammasome axis in coagulation, we assessed key thrombotic markers in monocytes. Hypoxia or DMOG exposure significant

increased microparticle-associated Tissue Factor (TF) activity (p=5.8E-10), TF protein (p=8.4E-6) and mRNA levels (p=9.0E-13) along with FVII expression (Figure 3A-C, S5). In the presence of DIM, MCC950 and SML0499, expression of these molecules was reduced. Activation of the extrinsic pathway of coagulation cascade to promote thrombogenesis leads to the regulation of the fibrinolytic system.[22] Consistent with a prothrombotic phenotype, we also observed changes in the fibrinolytic system. In sync with it, under hypoxia and DMOG treatment, there was an elevated expression of PAI-1 and reduced expression of uPA and tPA. These outcomes were reversed by DIM, MCC950 and SML0499 (Figure 3D-F). Similarly, in hPBMCs, TF and Factor VII were upregulated under hypoxia and DMOG which was suppressed by pharmacological inhibition of HIF-1α-NLRP3 axis confirming regulation of TF through this axis (Figure S4A). Following the demonstration of inflammation-mediated coagulation under hypoxia through this axis, we proceeded to analyze the downstream molecules of NLRP3 and coagulation trigger, TF, and its activity. We aimed to validate whether the activation of coagulation is interdependent with the release of cytokines IL-1β, Egr-1, and TF activity or not. Hence, we studied the correlation of the protein expression of HIF-1α vs. NLRP3, NLRP3 vs. IL-1β and IL-1β vs. Egr-1, and finally Egr-1 vs. tissue factor activity (Figure S6 A-D).

To specifically validate the role of Egr-1 as the key intermediary linking inflammation to coagulation, we employed an siRNA-mediated knockdown approach. First, we confirmed our proposed pathway hierarchy i.e., siRNA knockdown of upstream HIF-1α or NLRP3 each resulted in significantly lower Egr-1 expression (Figure S7 A-F). Next, we performed a critical experiment wherein the direct knockdown of Egr-1 led to a significant decrease in both TF mRNA expression (p=3.9E-9) and TF activity (p=4.7E-4) (Figure S7 G-H). Finally, to confirm the pathway directionality, we showed that Egr-1 knockdown had no effect on the upstream inflammasome components, as the expression of NLRP3, Caspase-1, and IL-1β remained unchanged (Figure S7 B-D). Taken together, this data provides robust evidence that Egr-1 functions as the critical downstream effector of the HIF-1α-NLRP3 axis to directly drive the expression of Tissue Factor.

**Functional role of platelet regulating thromboinflammation in monocytes through HIF-1α-NLRP3-Egr-1 axis**

Our observation that monocytes affect inflammation-mediated coagulation through the HIF-1α-NLRP3-Egr-1 axis prompted us to investigate the role of platelets in this process. While previous studies have established that hypoxia triggers platelet hyperactivation, leading to inflammation, enhanced aggregation, and thrombus stability,[23-27] the precise mechanism driving this hyperactivation is largely unexplored. Hence, we performed an *in vitro* investigation to determine if HIF-1α-NLRP3 inflammasome axis is responsible for this phenomenon. We measured the primary steps of platelet function like adhesion, aggregation and calcium release in hypoxia. Platelets exposed to hypoxia, DMOG demonstrated enhanced adhesion to collagen (Figure 4A), increased the rate and extent of platelet aggregation (Figure 4B, C) and stimulated calcium release (Figure 4D). Remarkably, this platelet hyperreactivity was significantly reduced by pharmacological inhibitors DIM, MCC950, and SML0499 (Figure 4A-D). Thus, this data supports the notion of platelet hyperreactivity being mediated through HIF-1α-NLRP3 inflammasome axis.

Furthermore, since this axis regulates platelet hyperreactivity and platelet–immune cell interactions influence inflammation-driven coagulation, it is important to study how platelets affect NLRP3-mediated coagulation in monocytes and macrophages. For this, we studied this axis in co-culture model of monocytes and platelets. We observed a significant increase in protein levels of HIF-1α, NLRP3, and IL-1β under hypoxia or DMOG treatment in comparison to platelet only group (activated platelets and monocytes with no exposure) (Figure 5A-B, S8). A similar pattern of increase was observed in mRNA transcripts of these molecules along with Egr-1 and Tissue Factor (Figure S8). With the inflammatory role, there was increased expression of Egr-1 protein (p=2.4E-6, p=4.6E-6), MPs-bound tissue factor activity (p=6.9E-13), mRNA expression of TF (p=7.6E-13), and FVII.) (Figure 5C-D, S8). Pharmacological inhibition of HIF-1α, NLRP3, and Caspase-1 decreased the expression of the molecules on this axis. Interestingly, addition of activated platelets to monocytes with no exposure significantly elevates mRNA expression compared to NA (monocytes only).

The interaction of monocytes to endothelial cells in presence of platelets showed a significant increased tissue factor activity in comparison to monocytes alone which is subsidize by inhibiting HIF-1α, NLRP3, caspase-1. This confirms that the system together aggravates the inflammation mediated coagulation (Figure S9). Thus, platelets act as amplifiers of the HIF-1α-NLRP3-Egr-1-TF axis in monocytes, resulting in a potent thromboinflammatory state.

**Validation of HIF-1α-NLRP3-Egr-1 axis involvement contributes to TF expression in the *in vivo* $FeCl_3$ thrombosis model**

After the association of the HIF-1α-NLRP3-Egr-1 axis promoting thromboinflammation *in vitro*, we next sought to validate the involvement of this axis in inflammation-mediated coagulation through the expression of TF in rat model. *In situ* examination of inferior vena cava (IVC) revealed a significantly heavier, and larger thrombus respectively in $FeCl_3$ (p=7.4E-11, p=7.6E-13), and DMOG-treated rats (p=7.6E-13, p=7.6E-13). A reduction in thrombus weight and size was observed in DIM (p=9.7E-12, p=9.7E-12), MCC950 (p=8.4E-13, p=8.4E-13) and SML0499 (p=7.6E-13, p=7.6E-13) (Figure 6A-C). The denser and heavier thrombus suggests the exaggerated thrombogenesis with the HIF-1α-NLRP3 axis.

Consistent with these physical findings, we investigated the systemic coagulation parameters and observed significantly shortened bleeding time (BT) (Figure 6D), activated partial thromboplastin time (aPTT), and prothrombin time (PT) (Figure S10) in DMOG and extended BT, aPTT and PT in DIM, MCC950 and SML0499 imply the role of the HIF-1α and NLRP3 in hypoxia-associated thrombogenesis.

Platelets play a significant role in thrombogenesis; hence we next analyzed platelet function ex vivo from the treated animals. Platelets isolated from exposed animals demonstrated enhanced adhesion (Figure S10) and increased rate extent of aggregation with time-dependent ADP induced in $Fecl_3$ and DMOG and reduced adhesion and decreased aggregation extent in DIM, MCC950 and SML0499 (Figure S10). Next, we observed a significant reduction in the release of eNOS in $FeCl_3$ (p=2.0E-6) and DMOG (p=4.2E-10) which increased in DIM, MCC950 and SML0499. This regulation of eNOS depicts platelets hyperactivation is facilitated by HIF-1α-NLRP3 axis promoting thrombus formation (Figure S10). Immunohistochemistry of the liver section further confirm an increased expression of Tissue Factor in the prothrombotic groups (Figure 6E). To further establish the association between proinflammatory and prothrombotic state, RNA and plasma were isolated from whole blood. We have observed increased mRNA transcripts and protein levels of HIF-1α, NLRP3, and its associated molecules such as Caspase-1, IL-1β, along with Egr-1, and TF in $FeCl_3$ and DMOG-treated rats, which were down-regulated in

DIM, MCC950 and SML0499 (Figure S11). This further validates the association of HIF-1α-NLRP3 axis in inflammation-mediated coagulation via HIF-α-NLRP3-Egr-1-TF axis.

**Involvement of the HIF-1α-NLRP3-Egr1-TF axis in high altitude induced DVT patients**

After the *in vitro* and *in vivo* validation, we subsequently investigated the potential involvement of this axis in clinically proven DVT cases brought on by a hypobaric hypoxic environment. Table S1 displays the demographic, and clinical, characteristics of patients with DVT**.** To see the functional involvement of this HIF-1α-NLRP3-Egr1-TF axis in the pathogenesis of DVT, we observed elevated transcripts of HIF-1α, NLRP3, and Caspase-1, and IL-1β. Along with this the downstream effectors responsible for driving coagulation like Egr-1 (p=0.006), TF (p=0.003) and, FVII (p=0.002) in patients compared with healthy (Figure 7A-H) along with the protein level of Egr-1 (p=0.006) was also increased (Figure 7F). This clinical data strongly supports the involvement of the HIF-1α-NLRP3-Egr1-TF axis in the pathogenesis of DVT in individuals who have been exposed to high-altitude hypoxic conditions.

In contrast to high-altitude conditions, the HIF-1α-NLRP3-TF axis is not pronounced in low altitude human patients, as there is no significant change in Caspase-1, IL-1β, Egr-1, and TF expression. An elevated NLRP3 expression was observed in patients, that could be due to underlying infection or release of damage associated molecular patterns. However, activation of NLRP-3 did not translate into downstream activation of Egr-1 and TF, the key mediators that promote DVT development (data not shown).

**Discussion**

A state of localized hypoxia has emerged as a key factor in regulating thromboinflammation with the HIF-1α-NLRP3 axis acting as a critical regulator of cellular responses in both physiological adaptation and pathological progression.[28-30] Since monocyte adhesion to the endothelial surface drives vascular inflammation represents a crucial therapeutic target for vascular diseases, including atherosclerosis.[31] The interaction between β2 integrin and JAM-1 facilitates transendothelial migration,[32] and monocytes adhesion to the endothelial surface. Our data demonstrates that the HIF-1α-NLRP3 axis facilitates the adhesion of monocytes to endothelial cells through β2 integrin and JAM-1/F11R under hypoxia- a process that is further amplified by

platelets. Therefore, inhibiting this axis has potential for treating vascular inflammation by reducing monocyte adherence.

Beyond β2 integrin's role in monocytes transition from anti-adhesive to pro-adhesive state, our studies revealed the role of NLRP3 inflammasome in regulating thromboinflammation under hypoxia.[5] Systemic inflammation strongly promotes thrombosis through increased pro-coagulant factors expression, inhibition of natural anticoagulants, reduced fibrinolytic activity, and enhanced platelet reactivity.[33-34] We elucidated a molecular mechanism whereby hypoxia triggers thromboinflammation through the HIF-1α-NLRP3-Caspase-1-IL-1β-Egr1-TF/FVII axis activation. NLRP3 inflammasome is quite crucial for thrombosis in various diseases, such as atherosclerosis[35], different inflammatory diseases[34] such as inflammatory bowel syndrome, rheumatoid arthritis, systemic lupus erythematosus, hypoxia[36], ischemic stroke[37], and SARS-COV2 infection.[38]

We demonstrated that Egr-1, a pivotal molecule connecting inflammation and coagulation through tissue factor, increases under hypoxia. Yan *et al.* have reported that Egr-1 activation is essential for hypoxia-driven TF expression by binding promoter regions and enhancing its transcription.[39] Our study provides additional information, showing that the regulation of thromboinflammation is mediated by HIF-1α-NLRP3 axis under hypoxia involving monocytes, platelets and endothelial cells. Previous study showed that monocytes/macrophages as primary TF sources after NLRP3 inflammasome activation, despite TF is produced in various cell types.[40] In addition to the activation of the extrinsic pathway of coagulation cascade, we observed dysregulation of fibrinolytic system. These findings suggest the HIF-1α-NLRP3 axis drives hypoxia-induced thrombosis by simultaneously modulating both extrinsic pathway of coagulation and fibrinolytic system, Egr-1 and TF amplification. To identify the possible mechanism, we observed that the HIF-1α-NLRP3-Egr-1 axis is highly correlated with tissue factor activity, thereby, promoting thrombosis. The abrogation of HIF-1α-NLRP3 axis attenuated hypoxia-induced thrombosis progression, further confirming the contribution of this axis and establishing an association between inflammation-mediated thrombosis via Egr-1. Although different research has proven the potential involvement of Egr-1 in triggering TF expression,[16-17] we postulate HIF-1α-NLRP3 inflammasome involvement in hypoxia-induced coagulation through IL-1β and Egr-1.

We next demonstrated the involvement of NLRP3 in platelet hyperreactivity and thromboinflammation. Beyond hemostatic activities, platelets modulate the inflammatory response by secreting pro-inflammatory mediators, initiating NETosis, and forming heterotypic leukocytes aggregates.[41-42] Along with other findings, the HIF-1α-NLRP3 axis increases platelet adhesion, aggregation and aggravates thromboinflammation, which is suppressed by inhibiting this axis. Other studies have shown that a deficiency of platelets' NLRP3 and IL-1β impairs clot retraction and in the context of sickle cell disease, reduces aggregation due to decreased P-selectin, and ATP release, thereby further attenuating thrombosis.[43-44]

We have demonstrated that Egr-1 promotes inflammation-mediated coagulation through the HIF-1α-NLRP3-IL-1β-Egr-1, and TF pathways, and this effect is further potentiated by platelets. Some studies have suggested platelets- monocytes interaction is mediated by protease-activated receptors (PAR1 and PAR2) and TF in Covid-19 contributes to the escalation of thromboinflammation and cytokine release.[45,46] The cytokines released from monocytes are promoted by activated platelets, highlighting the significance of platelet-monocyte aggregates in inflammatory response.[42] This interaction is reciprocal as platelets activate monocytes which further stimulate platelets, thus this crosstalk exacerbates the inflammatory response.[45,46] Hence, we postulate that platelets amplify thromboinflammation through platelet-monocyte/macrophages interactions, increasing the production of cytokines, and Egr-1 by monocytes through the HIF-1α-NLRP3-Egr-1 axis.

Consistent with our findings, various groups have demonstrated that platelets amplify inflammation in rheumatoid arthritis, through IL-1β. Recent studies showed platelets exhibited pro-atherogenic effects by inducing monocyte differentiation into pro-inflammatory macrophage phenotypes.[47,48] These observations support a broader role of platelet–monocyte interactions in vascular inflammation. However, further investigation is required to identify the platelet factors that boost the inflammasome activation in monocytes that further aggravate thrombogenesis.

## References


1. Tsao CW, Aday AW, Almarzooq ZI, et al. American Heart Association Council on Epidemiology and Prevention Statistics Committee and Stroke Statistics Subcommittee 2023; Heart Disease and Stroke Statistics-2023 Update: A Report from the American Heart Association. Circulation. 2023;147(8):e93-e621.
2. Coombes R. Venous thromboembolism caused 25,000 deaths a year, say MPs. BMJ. 2005;330(7491):559.
3. Lutsey PL, Zakai NA. Epidemiology and prevention of venous thromboembolism. Nat Rev Cardiol. 2023;20(4):248-262.
4. Braekkan SK, Hansen JB. VTE epidemiology and challenges for VTE prevention at the population level. Thromb Update. 2023;10:100132.
5. Lopez JA, Chen J. Pathophysiology of venous thrombosis. Thromb Res. 2009;123 Suppl 4:S30-34.
6. Gupta N, Sahu A, Prabhakar A, et al. Activation of NLRP3 inflammasome complex potentiates venous thrombosis in response to hypoxia. Proc Natl Acad Sci U S A. 2017;114(18):4763-4768.
7. Brill A, Suidan GL, Wagner DD. Hypoxia, such as encountered at high altitude, promotes deep vein thrombosis in mice. J Thromb Haemost. 2013;11(9):1773-1775.
8. Gupta N, Ashraf MZ. Exposure to high altitude: a risk factor for venous thromboembolism? Semin Thromb Hemost. 2012; 38(2):156-163.
9. Mannucci PM, Gringeri A, Peyvandi F, Di Paolantonio T, Mariani G. Short-term exposure to high altitude causes coagulation activation and inhibits fibrinolysis. Thromb Haemost. 2002;87(2):342-343.
10. Eltzschig HK, Carmeliet P. Hypoxia and inflammation. N Engl J Med. 2011;364(7):656-665.
11. von Bruhl ML, Stark K, Steinhart A, et al. Monocytes, neutrophils, and platelets cooperate to initiate and propagate venous thrombosis in mice in vivo. J Exp Med. 2012;209(4):819-835.
12. Scridon A. Platelets and Their Role in Hemostasis and Thrombosis-From Physiology to Pathophysiology and Therapeutic Implications. Int J Mol Sci. 2022; 23(21):12772.

13. Rayes J, Bourne JH, Brill A, Watson SP. The dual role of platelet-innate immune cell interactions in thrombo-inflammation. Res Pract Thromb Haemost. 2019;4(1):23-35.
14. Schulz C, Engelmann B, Massberg S. Crossroads of coagulation and innate immunity: the case of deep vein thrombosis. Journal of thrombosis and haemostasis: JTH. 2013;11 Suppl 1:233-241.
15. Rolfes V, Ribeiro LS, Hawwari I, et al. Platelets Fuel the Inflammasome Activation of Innate Immune Cells. Cell Rep. 2020;31(6):107615.
16. Pawlinski R, Pedersen B, Kehrle B, et al. Regulation of tissue factor and inflammatory mediators by Egr-1 in a mouse endotoxemia model. Blood. 2003;101(10):3940-3947.
17. Wu SQ, Minami T, Donovan DJ, Aird WC. The proximal serum response element in the Egr-1 promoter mediates response to thrombin in primary human endothelial cells. Blood. 2002;100(13):4454-4461.
18. Li W, Nieman M, Sen Gupta A. Ferric Chloride-induced Murine Thrombosis Models. J Vis Exp. 2016;(115):54479.
19. Cejkova S, Kralova-Lesna I, Poledne R. Monocyte adhesion to the endothelium is an initial stage of atherosclerosis development. Cor et Vasa. 2016;58(4):e419-425.
20. Mazzone A, Ricevuti G. Leukocyte CD11/CD18 integrins: biological and clinical relevance. Haematologica. 1995;80(2):161-175.
21. Czubak-Prowizor K, Babinska A, Swiatkowska M. The F11 Receptor (F11R)/Junctional Adhesion Molecule-A (JAM-A) (F11R/JAM-A) in cancer progression. Mol Cell Biochem. 2022;477(1):79-98.
22. Nair V, Singh S, Ashraf MZ, et al. Epidemiology and pathophysiology of vascular thrombosis in acclimatized lowlanders at high altitude: A prospective longitudinal study. Lancet Reg Health Southeast Asia. 2022;3:100016.
23. Delaney C, Davizon-Castillo P, Allawzi A, et al. Platelet activation contributes to hypoxia-induced inflammation. Am J Physiol Lung Cell Mol Physiol. 2021;320(3):L413-L421.
24. Cameron SJ, Mix DS, Ture SK, et al. Hypoxia and Ischemia Promote a Maladaptive Platelet Phenotype. Arterioscler Thromb Vasc Biol. 2018;38(7):1594-1606.

25. Chaurasia SN, Kushwaha G, Kulkarni PP, et al. Platelet HIF-2α promotes thrombogenicity through PAI-1 synthesis and extracellular vesicle release. Haematologica. 2019;104(12):2482-2492.
26. Tyagi T, Ahmad S, Gupta N, et al. Altered expression of platelet proteins and calpain activity mediate hypoxia-induced prothrombotic phenotype. Blood. 2014;123(8):1250-1260.
27. Prchal JT. Hypoxia and thrombosis. Blood. 2018;132(4):348-349.
28. Yang Y, Wang H, Kouadir M, Song H, Shi F. Recent advances in the mechanisms of NLRP3 inflammasome activation and its inhibitors. Cell Death Dis. 2019;10(2):128.
29. Kokura S, Yoshida N, Yoshikawa T. Anoxia/reoxygenation-induced leukocyte-endothelial cell interactions. Free Rad Biol Med. 2002;33(4):427-432.
30. Chanchal S, Mishra A, Singh MK, Ashraf MZ. Understanding Inflammatory Responses in the Manifestation of Prothrombotic Phenotypes. Front Cell Dev Biol. 2020;8:73.
31. Wang Y, Song E, Bai B, Vanhoutte PM. Toll-like receptors mediating vascular malfunction: Lessons from receptor subtypes. Pharmacol Ther. 2016;158:91-100.
32. Ostermann G, Weber KS, Zernecke A, Schröder A, Weber C. JAM-1 is a ligand of the beta(2) integrin LFA-1 involved in transendothelial migration of leukocytes. Nat Immunol. 2002;3(2):151-158.
33. Aksu K, Donmez A, Keser G. Inflammation-induced thrombosis: mechanisms, disease associations and management. Curr Pharm Des. 2012;18(11):1478-1493.
34. Esmon CT. Inflammation and thrombosis. J Thromb Haemost. 2003;1(7):1343-1348.
35. Puhlmann M, Weinreich DM, Farma JM, Carroll NM, Turner EM, Alexander HR, Jr. Interleukin-1beta induced vascular permeability is dependent on induction of endothelial tissue factor (TF) activity. J Transl Med. 2005;3:37.
36. Langer F, Spath B, Fischer C, et al. Rapid activation of monocyte tissue factor by antithymocyte globulin is dependent on complement and protein disulfide isomerase. Blood. 2013;121(12):2324-2335.
37. Levi M, van der Poll T. Inflammation and coagulation. Crit Care Med. 2010;38(2 Suppl):S26-S34.
38. Avila J, Long B, Holladay D, Gottlieb M. Thrombotic complications of COVID-19. Am J Emerg Med. 2021; 39:213-218.

39. Yan SF, Zou YS, Gao Y, et al. Tissue factor transcription driven by Egr-1 is a critical mechanism of murine pulmonary fibrin deposition in hypoxia. Proc Natl Acad Sci U S A. 1998;95(14):8298-8303.
40. Grover SP, Mackman N. Tissue Factor: An Essential Mediator of Hemostasis and Trigger of Thrombosis. Arterioscler Thromb Vasc Biol. 2018;38(4):709-725.
41. Martinod K, Wagner DD. Thrombosis: tangled up in NETs. Blood. 2014;123(18):2768-2776.
42. Franco AT, Corken A, Ware J. Platelets at the interface of thrombosis, inflammation, and cancer. Blood. 2015;126(5):582-588.
43. Qiao J, Wu X, Luo Q, et al. NLRP3 regulates platelet integrin αIIbβ3 outside-in signaling, hemostasis and arterial thrombosis. Haematologica. 2018;103(9):1568-1576.
44. Vogel S, Kamimura S, Arora T, et al. NLRP3 inflammasome and bruton tyrosine kinase inhibition interferes with upregulated platelet aggregation and in vitro thrombus formation in sickle cell mice. Biochem Biophys Res Commun. 2021;555:196-201.
45. Hottz ED, Martins-Gonçalves R, Palhinha L, et al. Platelet-monocyte interaction amplifies thromboinflammation through tissue factor signaling in COVID-19. Blood Adv. 2022;6(17):5085-5099.
46. Hottz ED, Azevedo-Quintanilha IG, Palhinha L, et al; Platelet activation and platelet-monocyte aggregate formation trigger tissue factor expression in patients with severe COVID-19. Blood. 2020;136(11):1330-1341.
47. Boilard E, Nigrovic PA, Larabee K, et al. Platelets amplify inflammation in arthritis via collagen-dependent microparticle production. Science. 2010;327(5965):580-583.
48. Barrett TJ, Schlegel M, Zhou F, et al. Platelet regulation of myeloid suppressor of cytokine signaling 3 accelerates atherosclerosis. Sci Transl Med. 2019;11(517):eaax0481.

**Figure Legends**

**Figure 1: Adherence of monocytes to endothelial cells.**

Endothelial cells (ECs) were exposed to hypoxia for 8h for all the experimental conditions to create endothelium surface and simultaneously THP-1 cells (Monocytes) were exposed to hypoxia for 8 h, HIF-1α activator-Dimethyloxalylglycine (DMOG) for 12h, DMOG + HIF-1α inhibitor-DIM, NLRP3 inhibitor-MCC950+DMOG and the inhibitor of catalytic activity of Caspase-1-SML0499+DMOG. All the inhibitors were used for 4h each. Adherence was subsequently determined in all the experimental conditions (Comparison was done No addition (NA) vs. Hypoxia and DMOG; DMOG vs. DIM, MCC950, and SML0499). **A,** Number of monocytes adhere to endothelial cells; **B,** Effect of platelets on the number of monocytes adherence to endothelial cells. Differentiated and ADP activated megakaryocytic cells were added to monocytes and ECs in all the above-mentioned experimental conditions; **C,** Expression of β2 integrin adhesion molecules on the co-culture of monocytes and endothelial cells; **D,** Involvement of F11R gene on the co-culture of monocytes and endothelial cells; **E,** Representation of adhesion of monocytes to endothelial cells in all the experimental conditions. Statistical analysis was performed using the One-way ANOVA with the Turkey multiple comparison test. Data is represented as SEM ±.

**Figure 2: Implication of hypoxia response pathway in the regulation of NLRP3 inflammasome axis and Identification of HIF-1α binding site in Egr-1 promoter.** Monocytes were treated to all the experimental conditions. RNA and whole cell lysate were collected. **Regulation of hypoxia response pathway**: **A,** Estimation of HIF-1α protein; **Hypoxia exposure results in a pro-inflammatory state through the HIF-1a-NLRP3 inflammasome axis**: **B-D,** Protein levels of NLRP3, IL-1β, and Egr-1 in all the experimental conditions (Comparison was done No addition (NA) vs. Hypoxia and DMOG; DMOG vs. DIM, MCC950, and SML0499. **E,** CHIP was used to examine HIF-1α binding to the Egr-1 promoter in normoxia, hypoxia, DMOG with and without HIF-1α inhibitor, NLRP3 inhibitor, and the inhibitor of catalytic activity of Caspase-1; **F,** Regions of Egr-1 promoter depicting the binding site of HIF-1α, spanning nucleotide at -1302 to -1295, -1585 to -1578, and -869 to-862, depicted is the HIF-1α binding site within the Egr-1 promoter having the sequence 5'-TCACGTCA-3'. Statistical analysis was

performed using the One-way ANOVA with the Turkey multiple comparison test. Data is represented as SEM ±.

**Figure 3: Hypoxia-induced prothrombotic state is regulated through HIF-1a-NLRP3 inflammasome axis.** Monocytes were treated to all the experimental conditions. RNA and whole cell lysate were collected: Expression of Tissue Factor (TF) in all the different experimental conditions indicating its regulation through this axis. **A,** Estimation of microparticles bound tissue factor activity (TFU); **B,** Expression of TF through flow cytometry; **C,** Quantification of TF positive cells under different experimental conditions. A total of 10,000 events were analyzed in triplicate; D-F, Activation of the fibrinolytic pathway under the influence of HIF-1α; **D,** Relative levels of PAI-1; **E,** uPA; **F,** tPA in all experimental conditions as described above. (Comparison was done with No addition (NA) versus Hypoxia and DMOG; DMOG versus DIM, MCC950, and SML0499. The expression of the gene was normalized with 18sRNA, as an internal control to that of the NA group. Statistical analysis was performed using the One-way ANOVA with the Turkey multiple comparison test. Data is represented as SEM ±.

**Figure 4. Functional activity of platelets under the influence of HIF-1α- NLRP3 inflammasome.** Differentiated and ADP activated megakaryocytic cells were stimulated and treated with all the experimental conditions: **A**, Adhesion of platelets to collagen in all different experimental conditions; **B**, Platelets percent aggregation under the influence of hypoxia through HIF-1a-NLRP3 axis; **C**, Kinetics of platelets aggregation showing increasing aggregation regulated by HIF-1a-NLRP3; **D**, Detection of intracellular platelets calcium indicating platelets function. (Comparison was done No addition (NA) versus Hypoxia and DMOG; DMOG verses DIM and MCC950); Statistical analysis was performed using the One-way ANOVA with the Turkey multiple comparison test (A, B, D) and Linear regression was used (C). Data is represented as SEM ±.

**Figure 5: Platelets strengthen the pro-inflammatory and pro-thrombotic milieu under hypoxia.** To see the effects of platelets on monocytes in inflammation-mediated coagulation: Monocytes without any treatment (NA), Monocytes with hypoxia for 8h (Hypoxia), Platelets without any treatment (NA'), ADP activated platelets (Platelets), Monocytes without any treatment and in the presence of activated platelets (Platelets'), Monocytes were stimulated with hypoxia for 8 h (Hypoxia'), DMOG for 12 h, DIM, MCC950, and SML0499 for 4 h each and co-

culture with ADP activated platelets. RNA and whole cell lysate were collected as per the experimental condition monocytes, platelets and co-culture of monocytes and ECs, respectively. Gene and protein levels were subsequently determined in all the above-mentioned experimental conditions. **A,** Protein levels of HIF-1α; **B,** Relative protein levels of NLPR3 ; **C,** Relative levels of Egr-1 protein level; and **D,** Microparticles bound tissue factor activityin all the experimental conditions as mentioned. Statistical analysis was performed using the One-way ANOVA with the Turkey multiple comparison test. Data is represented as SEM ±.

**Figure 6. Acceleration of venous thromboembolism through HIF-1α-NLRP3-Egr-1 axis. A,** Representation of heat maps of IVC thrombus in situ in all experimental conditions; **B,** Thrombus weight; **C,** Thrombus length; **D,** Bleeding time; **E,** Representation of hematoxylin-eosin-stained and Immunocytochemistry images of Liver cross section showing TF expression in all experimental conditions. Statistical analysis was performed using the One-way ANOVA with the Turkey multiple comparison test. Data is represented as SEM ±.

**Figure 7: Evidence for the involvement of the HIF-1α-NLRP3-Egr1-TF axis in high altitude-induced thrombotic human patients.** Total RNA was isolated and collected from whole blood samples of thrombotic patients (n=10), and gene expression was quantified. The expression of the gene was normalized with 18sRNA, as an internal control to that of the control; **A-F,** The relative expression of **A,** HIF-1α, **B,** NLRP3, **C,** Caspase-1, **D,** IL-1β, **E,** Egr-1, **F,** Egr-1 protein levels; **G,** F3; and **H,** F7 transcripts in thrombotic vs. control. *Statistical analysis was performed using unpaired Student t tests.* Data is represented as SEM ±. The Blue color indicates the mean value.

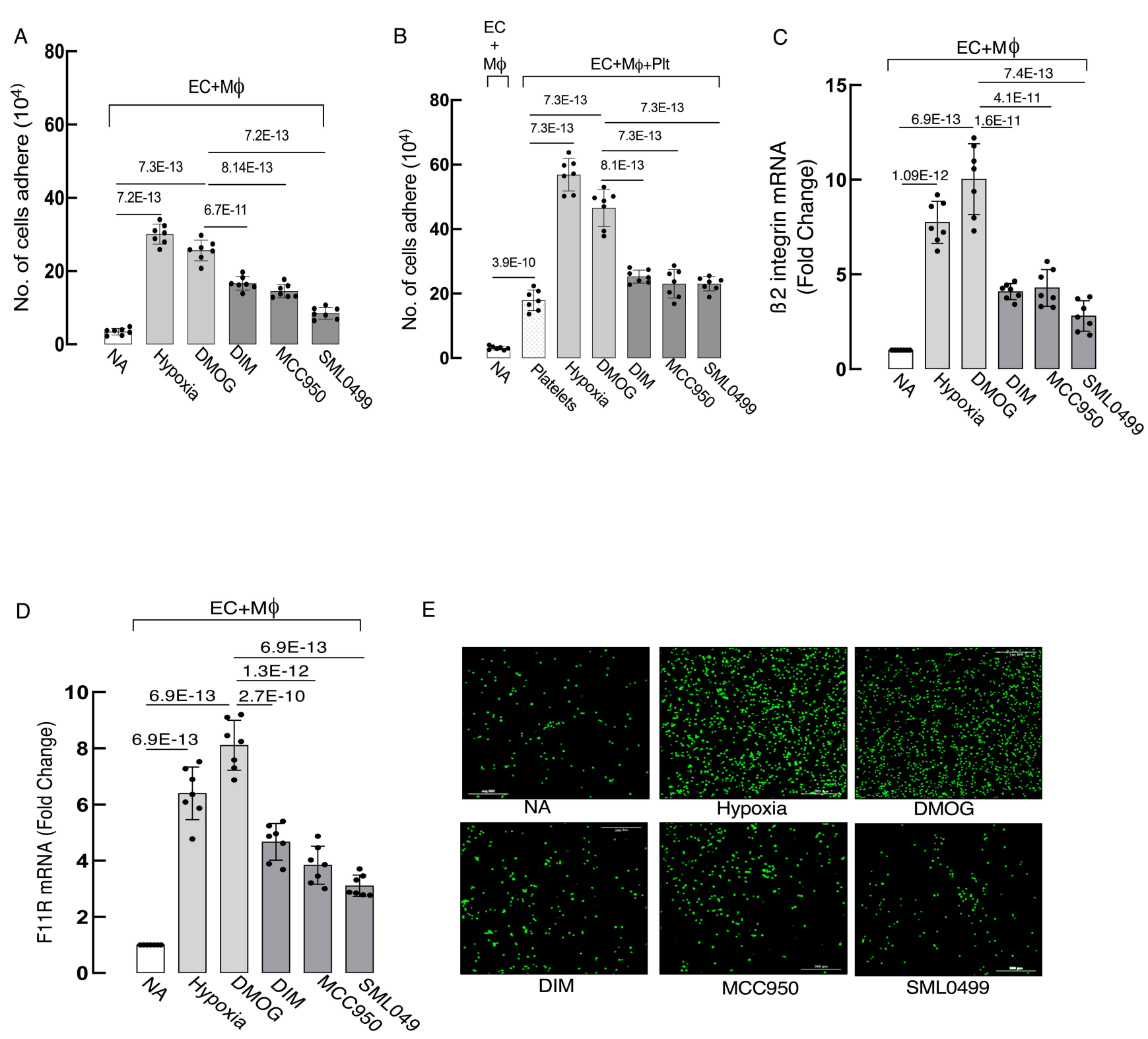
A
No. of cells adhere ($10^4$)
EC+Mϕ
7.2E-13
7.3E-13
8.14E-13
7.2E-13
6.7E-11
NA
Hypoxia
DMOG
DIM
MCC950
SML0499
B
EC + Mϕ
EC+Mϕ+Plt
7.3E-13
7.3E-13
7.3E-13
7.3E-13
8.1E-13
3.9E-10
NA
Platelets
Hypoxia
DMOG
DIM
MCC950
SML0499
C
EC+Mϕ
7.4E-13
4.1E-11
6.9E-13
1.6E-11
1.09E-12
β2 integrin mRNA (Fold Change)
NA
Hypoxia
DMOG
DIM
MCC950
SML0499
D
EC+Mϕ
6.9E-13
1.3E-12
6.9E-13
2.7E-10
6.9E-13
F11R mRNA (Fold Change)
NA
Hypoxia
DMOG
DIM
MCC950
SML049
E
NA
Hypoxia
DMOG
DIM
MCC950
SML0499

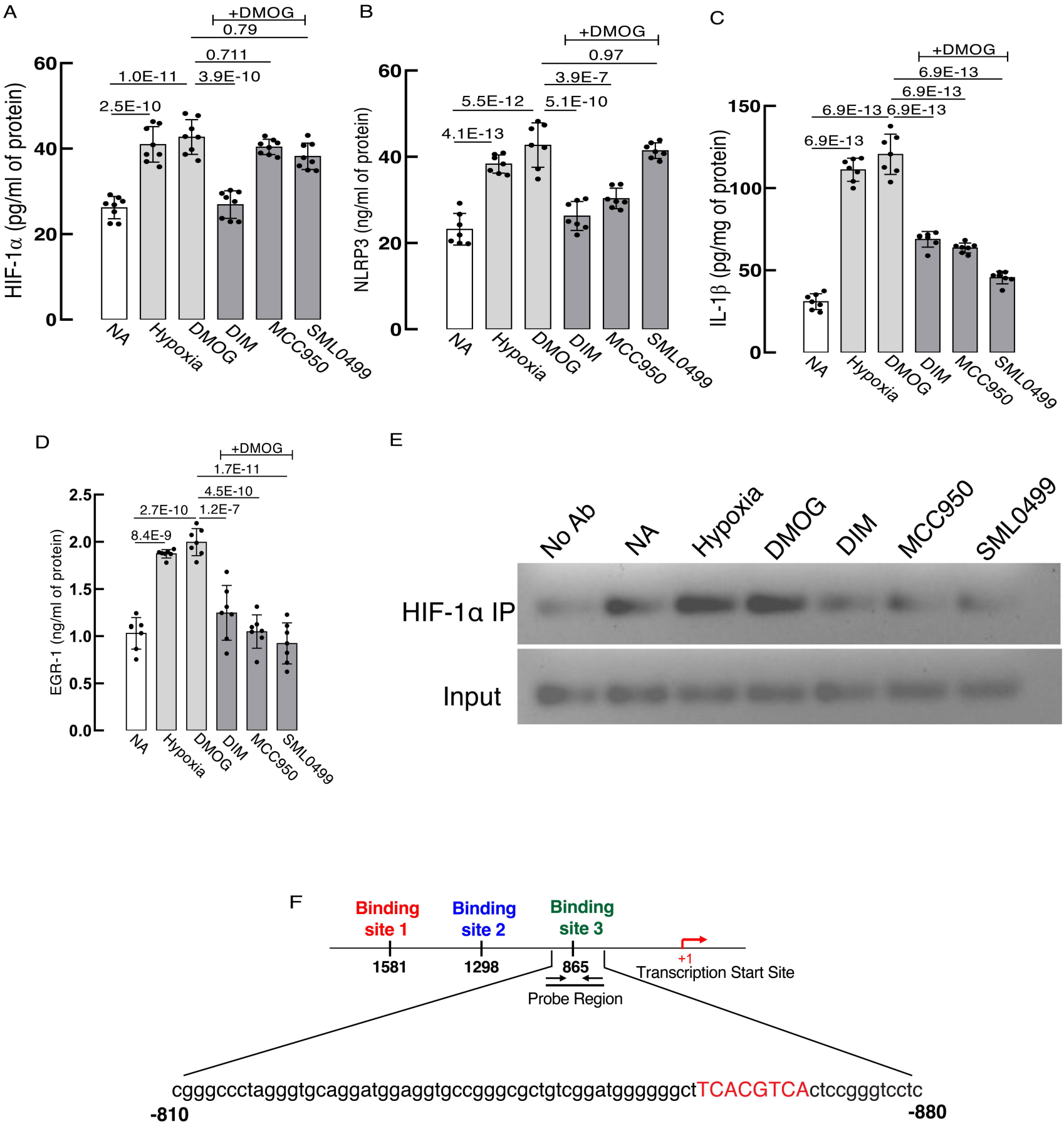
A
HIF-1α (pg/ml of protein)
+DMOG
0.79
0.711
1.0E-11
3.9E-10
2.5E-10
NA
Hypoxia
DMOG
DIM
MCC950
SML0499
B
NLRP3 (ng/ml of protein)
+DMOG
0.97
3.9E-7
5.5E-12
5.1E-10
4.1E-13
C
IL-1β (pg/mg of protein)
+DMOG
6.9E-13
6.9E-13
6.9E-13
6.9E-13
6.9E-13
D
EGR-1 (ng/ml of protein)
+DMOG
1.7E-11
4.5E-10
2.7E-10
1.2E-7
8.4E-9
E
No Ab
NA
Hypoxia
DMOG
DIM
MCC950
SML0499
HIF-1α IP
Input
F
Binding site 1
Binding site 2
Binding site 3
1581
1298
865
+1
Transcription Start Site
Probe Region
cgggccctagggtgcaggatggaggtgccgggcgctgtcggatgggggctTCACGTCActccgggtcctc
-810
-880

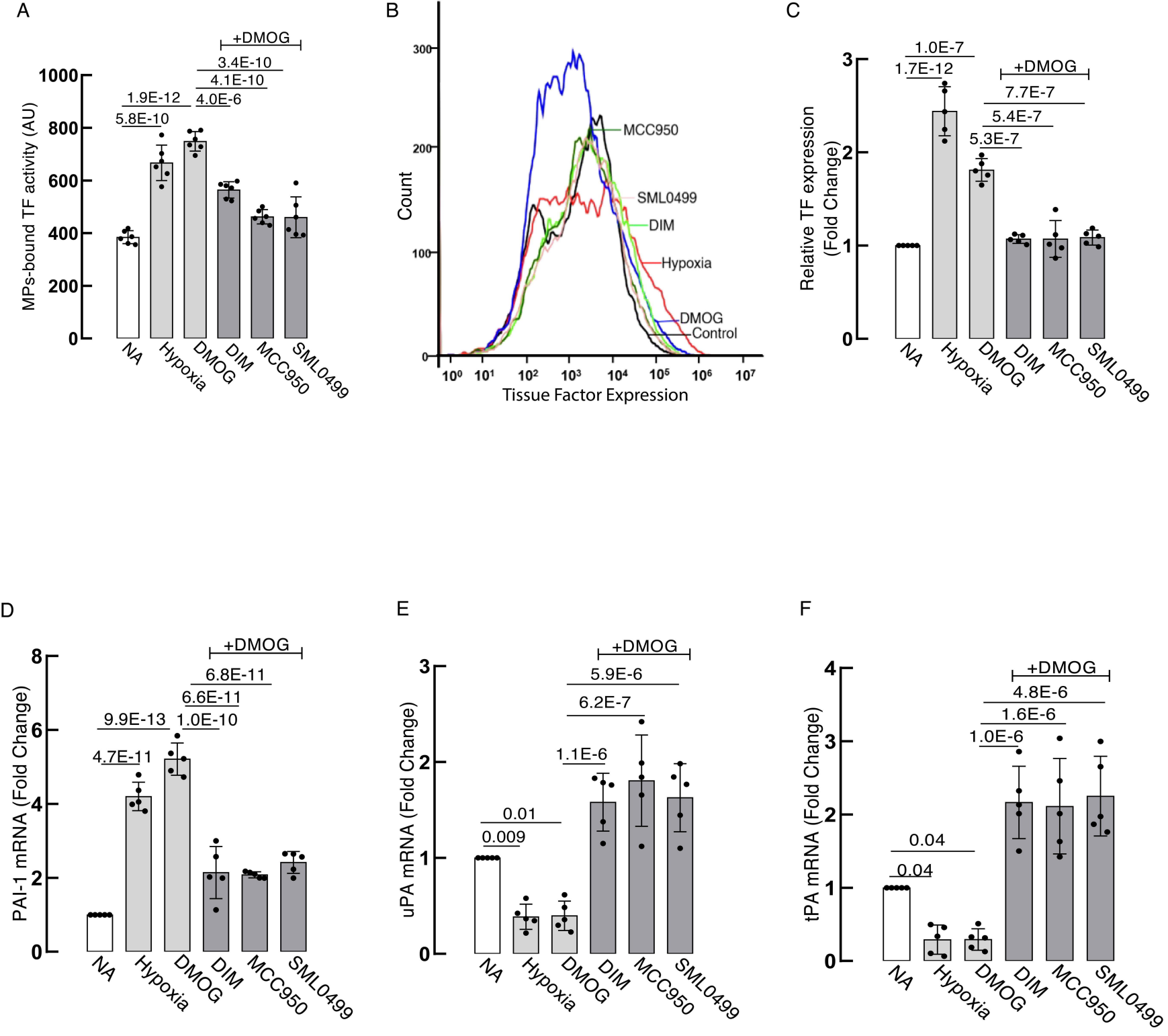
A
MPs-bound TF activity (AU)
1000
800
600
400
200
0
+DMOG
3.4E-10
4.1E-10
4.0E-6
1.9E-12
5.8E-10
NA
Hypoxia
DMOG
DIM
MCC950
SML0499
B
Count
300
200
100
0
MCC950
SML0499
DIM
Hypoxia
DMOG
Control
$10^0$ $10^1$ $10^2$ $10^3$ $10^4$ $10^5$ $10^6$ $10^7$
Tissue Factor Expression
C
Relative TF expression
(Fold Change)
3
2
1
0
1.0E-7
1.7E-12
+DMOG
7.7E-7
5.4E-7
5.3E-7
NA
Hypoxia
DMOG
DIM
MCC950
SML0499
D
PAI-1 mRNA (Fold Change)
8
6
4
2
0
+DMOG
6.8E-11
6.6E-11
9.9E-13
1.0E-10
4.7E-11
NA
Hypoxia
DMOG
DIM
MCC950
SML0499
E
uPA mRNA (Fold Change)
3
2
1
0
+DMOG
5.9E-6
6.2E-7
1.1E-6
0.01
0.009
NA
Hypoxia
DMOG
DIM
MCC950
SML0499
F
tPA mRNA (Fold Change)
4
3
2
1
0
+DMOG
4.8E-6
1.6E-6
1.0E-6
0.04
0.04
NA
Hypoxia
DMOG
DIM
MCC950
SML0499

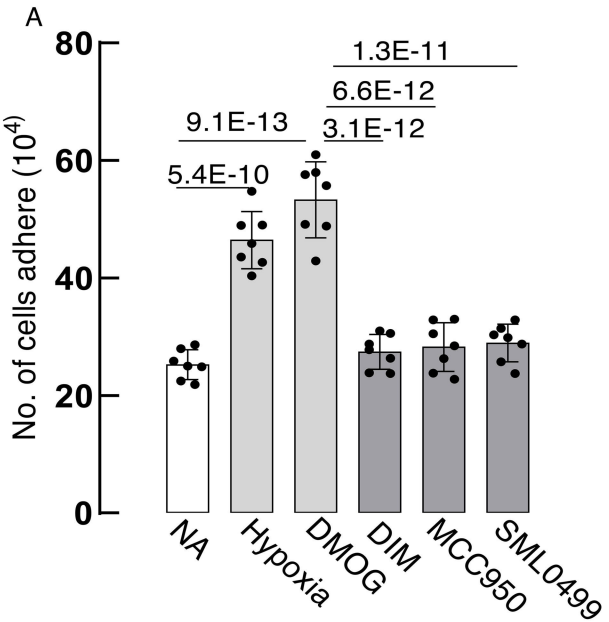
A
No. of cells adhere ($10^4$)
80
60
40
20
0
1.3E-11
6.6E-12
9.1E-13
3.1E-12
5.4E-10
NA
Hypoxia
DMOG
DIM
MCC950
SML0499

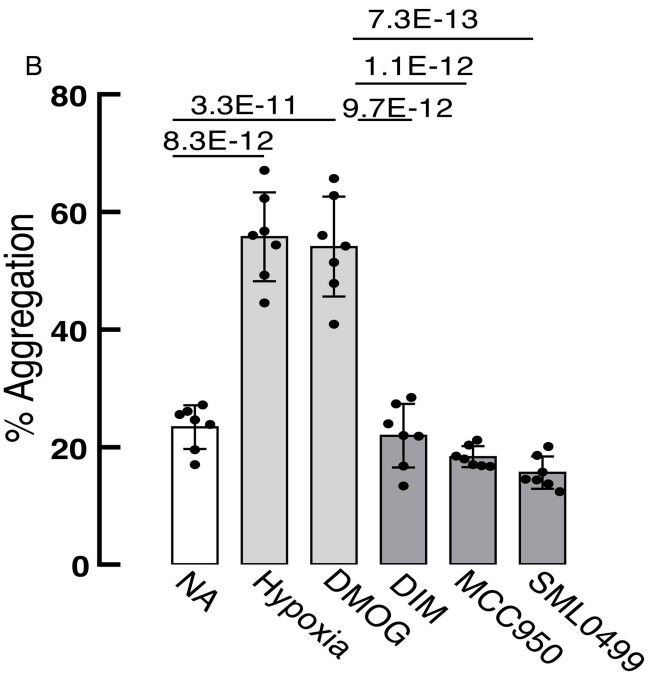
B
% Aggregation
80
60
40
20
0
7.3E-13
1.1E-12
3.3E-11
9.7E-12
8.3E-12
NA
Hypoxia
DMOG
DIM
MCC950
SML0499

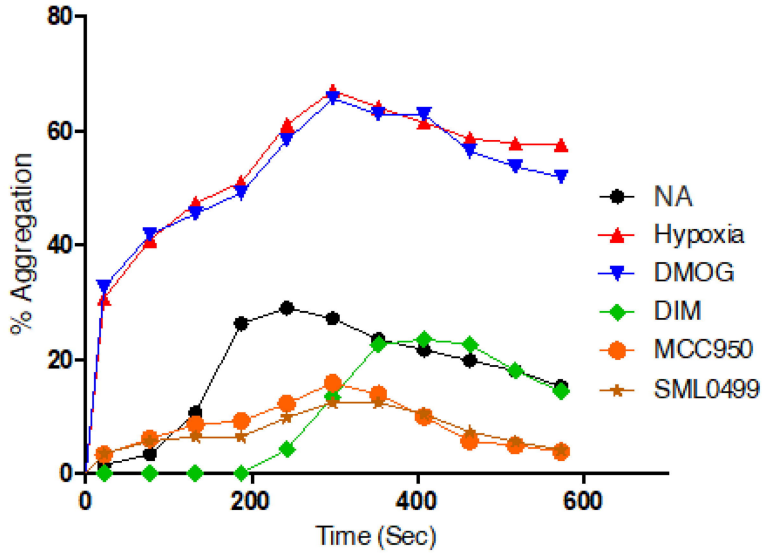
C
% Aggregation
80
60
40
20
0
0
200
400
600
Time (Sec)
NA
Hypoxia
DMOG
DIM
MCC950
SML0499

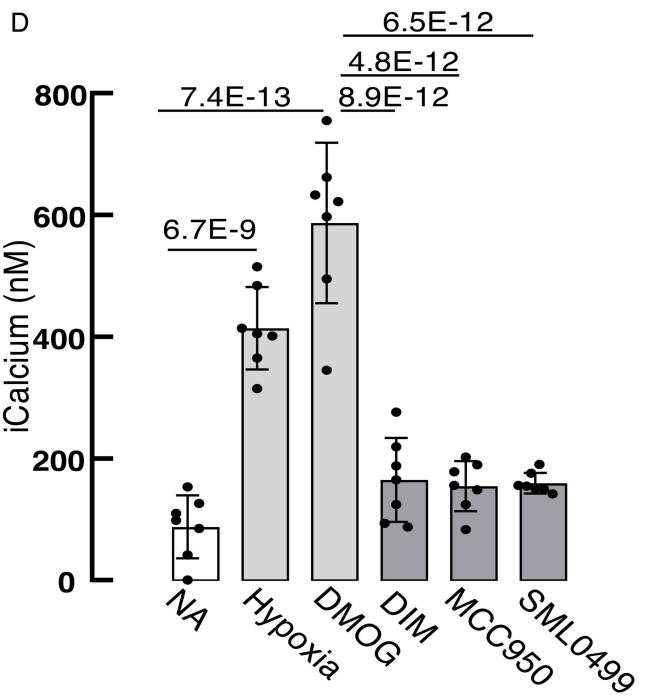
D
iCalcium (nM)
800
600
400
200
0
6.5E-12
4.8E-12
7.4E-13
8.9E-12
6.7E-9
NA
Hypoxia
DMOG
DIM
MCC950
SML0499

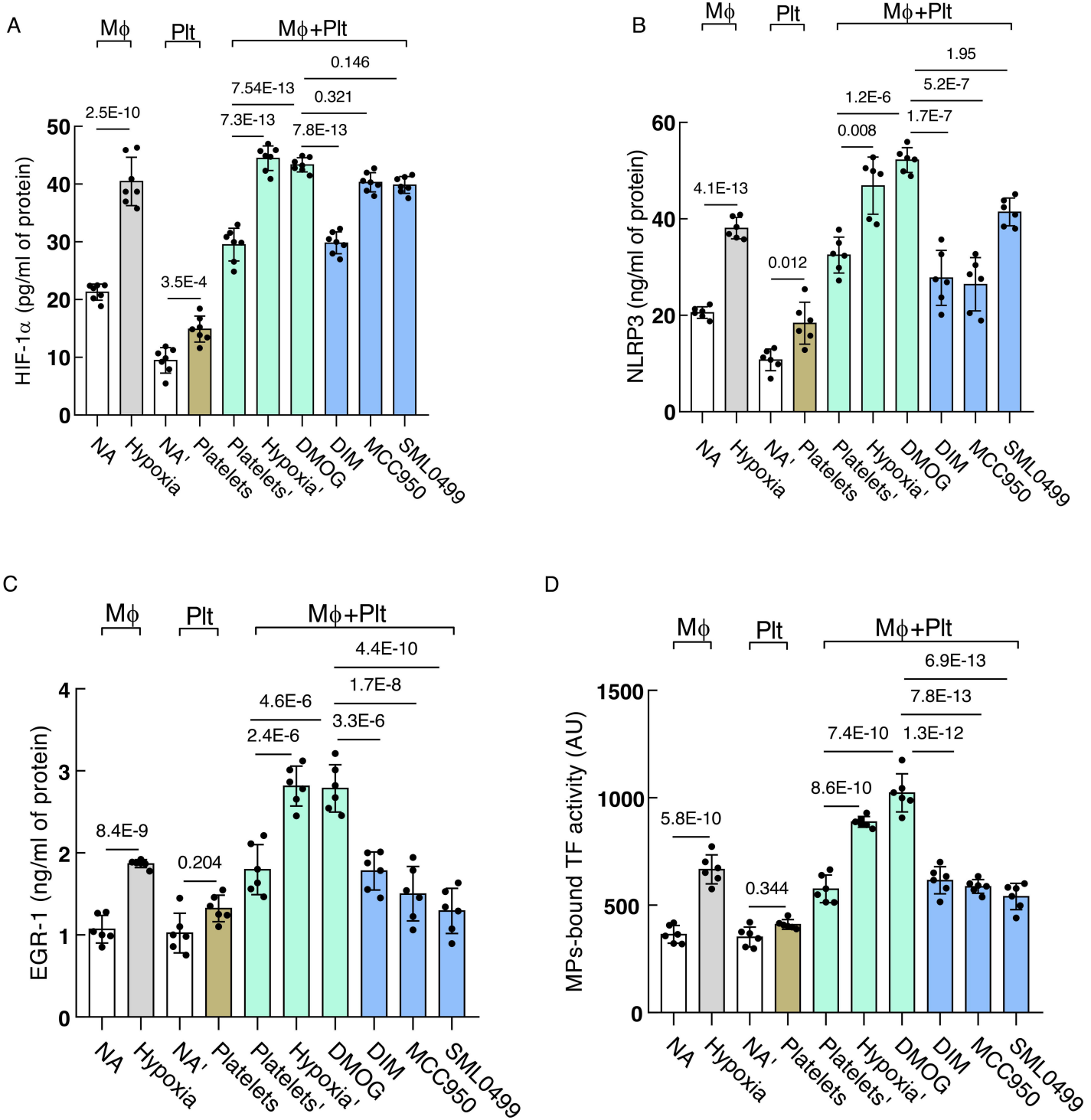
A
Mϕ
Plt
Mϕ+Plt
HIF-1α (pg/ml of protein)
2.5E-10
3.5E-4
7.3E-13
7.54E-13
0.321
7.8E-13
0.146
NA
Hypoxia
NA'
Platelets
Platelets'
Hypoxia'
DMOG
DIM
MCC950
SML0499
B
NLRP3 (ng/ml of protein)
4.1E-13
0.012
0.008
1.2E-6
1.7E-7
5.2E-7
1.95
C
EGR-1 (ng/ml of protein)
8.4E-9
0.204
2.4E-6
4.6E-6
3.3E-6
1.7E-8
4.4E-10
D
MPs-bound TF activity (AU)
5.8E-10
0.344
8.6E-10
7.4E-10
1.3E-12
7.8E-13
6.9E-13

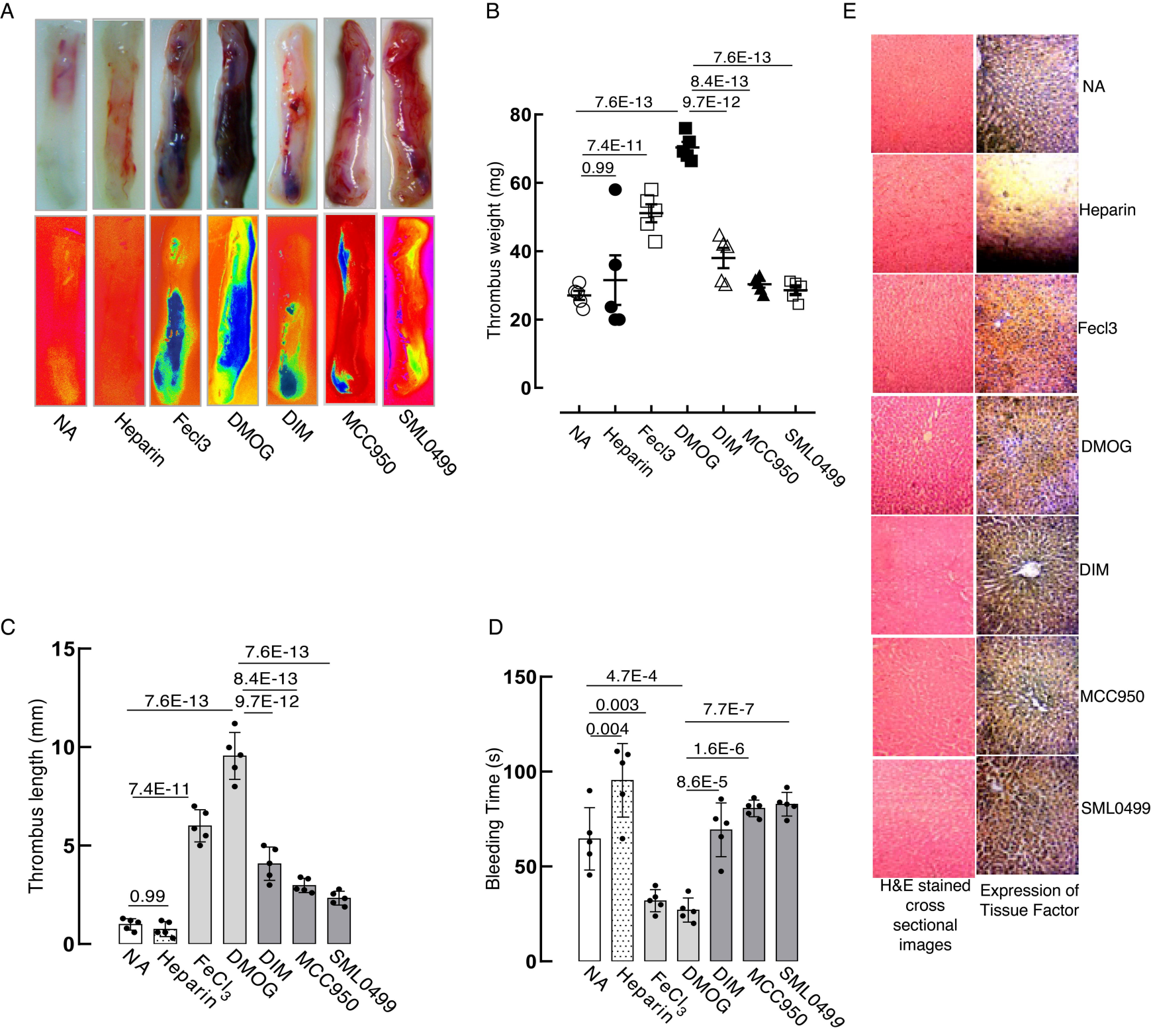
A
NA
Heparin
Fecl3
DMOG
DIM
MCC950
SML0499
B
Thrombus weight (mg)
0
20
40
60
80
7.6E-13
8.4E-13
9.7E-12
7.6E-13
7.4E-11
0.99
NA
Heparin
Fecl3
DMOG
DIM
MCC950
SML0499
C
Thrombus length (mm)
0
5
10
15
7.6E-13
8.4E-13
9.7E-12
7.6E-13
7.4E-11
0.99
NA
Heparin
FeCl3
DMOG
DIM
MCC950
SML0499
D
Bleeding Time (s)
0
50
100
150
4.7E-4
0.003
0.004
7.7E-7
1.6E-6
8.6E-5
NA
Heparin
FeCl3
DMOG
DIM
MCC950
SML0499
E
NA
Heparin
Fecl3
DMOG
DIM
MCC950
SML0499
H&E stained cross sectional images
Expression of Tissue Factor

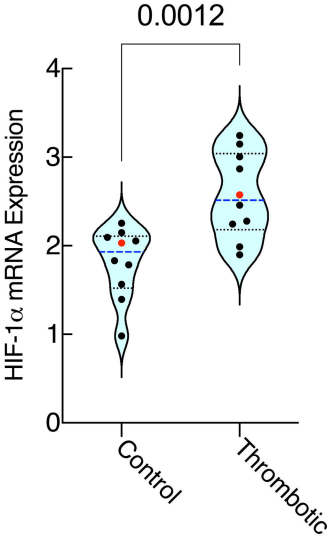
0.0012
HIF-1α mRNA Expression
0
1
2
3
4
Control
Thrombotic

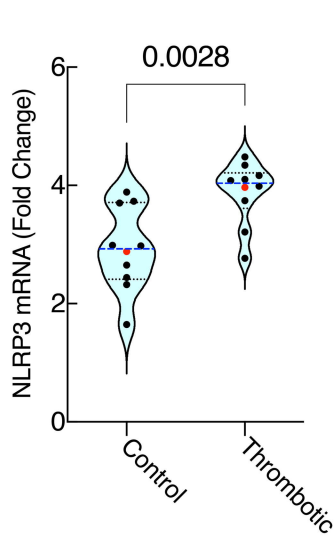
0.0028
NLRP3 mRNA (Fold Change)
0
2
4
6
Control
Thrombotic

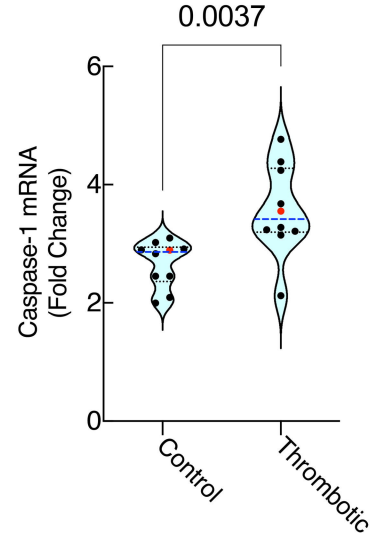
0.0037
Caspase-1 mRNA
(Fold Change)
0
2
4
6
Control
Thrombotic

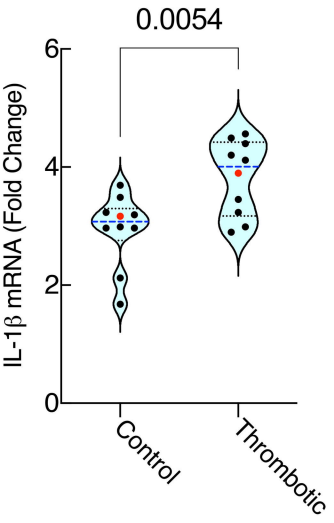
0.0054
IL-1β mRNA (Fold Change)
0
2
4
6
Control
Thrombotic

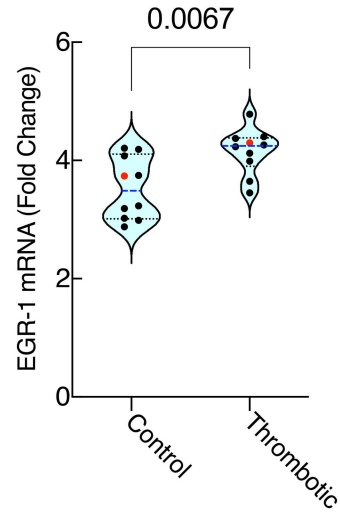
0.0067
EGR-1 mRNA (Fold Change)
0
2
4
6
Control
Thrombotic

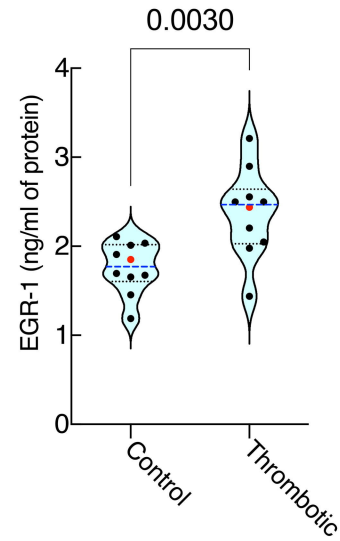
0.0030
EGR-1 (ng/ml of protein)
0
1
2
3
4
Control
Thrombotic

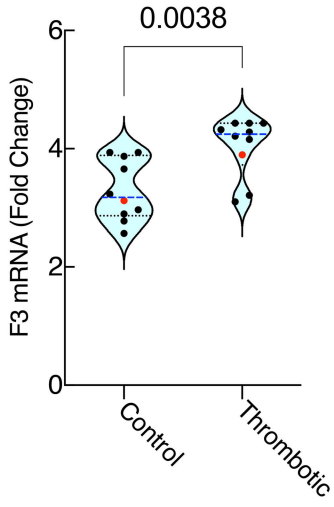
0.0038
F3 mRNA (Fold Change)
0
2
4
6
Control
Thrombotic

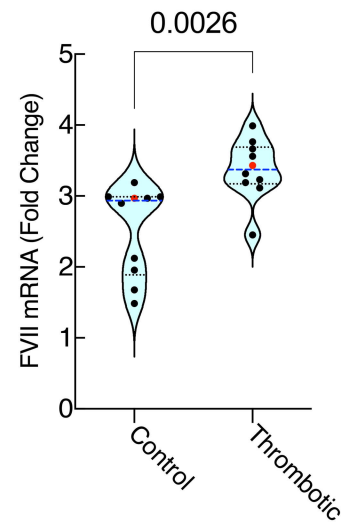
0.0026
FVII mRNA (Fold Change)
0
1
2
3
4
5
Control
Thrombotic

## SUPPLEMENTAL MATERIALS

### Detailed Methods

### Culturing, Maintaining Cell lines and their treatments

THP-1, the human leukemia monocytic cell line; K-562, the human myelogenous leukemia cell line was obtained from the National Centre for Cell Science (NCCS, Pune, India). It was cultured, and maintained in RPMI-1640 media which was supplemented with Fetal bovine serum (FBS)-10%, and penicillin-streptomycin (PS)-1% antibiotic- at a cell density of $0.5\times10^6$/ml and $3\times10^6$/ml respectively in a 5% $CO_2$ incubator at 37°C.[1] THP-1 were differentiated to macrophages with 20ηM PMA for 12 h and then replaced with fresh growth media for another 12 h before treatment.[2] The megakaryocytic differentiation of K-562 into platelets was done using 50 ηM PMA for 24 h and then replaced with 12 h before treatment.[1,3] The human umbilical vein cell line, Ea. hy926 was a kind gift from Central Drug Research Institute (CDRI), Lucknow, India, which was cultured, in DMEM media supplemented with 15% FBS and 1%PS antibiotic at a cell density of $1\times10^5$/ml at 37°C in a 5% $CO_2$ incubator. Human umbilical vein endothelial cells (HUVECs) were a kind gift from Institute of Genomics and Integrative Biology (IGIB), Delhi, India. HUVECs were maintained in Human Large Vessel Endothelial Cell Baαsal Medium supplemented with Low Serum Growth Supplement (LSGS). For isolation of hPBMCs, peripheral venous blood was collected from donors/patients at ESIC Medical College with the written informed consent and approval from the Institutional Ethics Committee of ESIC Medical College, Faridabad. Blood was drawn into sterile vacutainer tubes containing EDTA and processed within 2h of collection. Briefly, whole blood was diluted 1:1 with PBS in a 15ml falcon. The diluted blood was carefully layered over Histopaque® 1077 (MP Biomedicals) in a fresh 15 mL tube by slowly dispensing the sample down the tube wall to avoid mixing of layers. Samples were centrifuged at 400xg for 30 min at RT with the brake off. Following centrifugation, the PBMC layer appearing as a whitish, cloudy band at the plasma–Ficoll interface was carefully aspirated and transferred to a new tube. The harvested hPBMCs were washed twice with sterile PBS (300xg 5 min at RT) to remove residual platelets and Ficoll. The cell pellet was resuspended in RPMI-1640 medium (Gibco) supplemented with 2% heat-inactivated fetal bovine serum (FBS; Gibco) for cell counting and viability assessment. Freshly isolated hPBMCs were used immediately for downstream experiments.

**Monocyte endothelial Adhesion assay**

After experimental treatment, THP-1 cells or hPBMCs were incubated with 2′,7′- bis-(Carboxyethyl)-5(6′)-carboxyfluorescein Acetoxymethyl Ester (BCECF-AM) dye.[4] After internalization, the acetoxymethyl ester hydrolyzed, resulting in BCECF labeled cells. After Phosphate-buffered saline (PBS) washed twice, the labeled cells were added to activated endothelial cells (Ea. hy926 or HUVECs), subjected to hypoxia for 8 h, and incubated for 30 min at 37°C. After PBS washed, the fluorescence intensity was measured. The adherence of monocytes was extrapolated using standard curves produced by serially diluting a known number of labeled cells.

**Gene Expression/Transcriptional analysis**

In accordance with the manufacturer's instructions, total RNA was isolated from the all the cells and thrombosed IVC/whole blood samples using TRIzol reagent (Sigma-Aldrich). Briefly, an iScript cDNA synthesis kit (BioRad) was utilized to reverse-transcribe 1 µg of total RNA. SyBR Green (Thermo Fisher) for quantification of mRNA was used in quantitative real-time PCR machine (StepOne Real-Time PCR). Each gene's $C^t$ values were compared to the housekeeping 18sRNA for normalization, and the ΔΔCt method was utilized to determine the relative expression of each gene.

**Histopathological analysis**

Liver tissue samples from all the mentioned groups of animals were fixed in formalin solution and morphological assessment was done. These specimens underwent regular drying for the histological section, paraffin embedding, sectioning, and mounting on poly-lysine coated glass slides for the ensuing hematoxylin and eosin staining and TF immunohistochemistry analysis.

**Immunocytochemistry**

THP-1, the human monocytic cell line was stimulated to differentiate into macrophages induced with 20ηM PMA on coverslips coated with poly l-lysine (Sigma-Aldrich) at a cell density of $5\times10^5$. After 12 h of PMA induction, following 12 h in fresh media incubation. The cells were stimulated with experimental conditions. After PBST (PBS having tween20) wash thrice, the cells with the help of 4% paraformaldehyde fixed at room temperature (RT) for 15 min (Sigma-Aldrich). Two

consecutive washes with ice-cold PBS were then performed. After permeabilization with PBST (PBS containing Triton X-100-0.2%) for 10 min, the cells were washed thrice with PBS. Subsequently, with 5% BSA (Himedia) the cells were blocked for 30 min and incubated with primary antibodies against NLRP3 (1:200 dilution), and TF (1:200 dilution) in a humidified chamber at 4˚C with a gentle shaker. This was followed by PBS washing thrice for 5 min followed by incubation of the cells with Alexa Fluor 488, and Alexa Fluor 568 respectively tagged secondary antibody (Thermo Fisher Scientific, Inc.) for 1 hr at RT in the dark. Following a PBS wash, the cells were mounted on a glass slide with DAPI (ProLong™ Gold Antifade Mountant) on a glass slide and images were captured using fluorescence microscopy (ZOE Fluorescent Cell Imager, BioRad). The image J image analysis software was used to measure the intensity of each image, and the plot was made using Graphpad software.

**Enzyme-linked Immunosorbant assay (ELISA)**

To determine the activated HIF-1α, NLRP3 levels, cytokine IL-1β levels, Egr-1 and TF antigen in cell culture supernatants/lysates from leukocytes/monocytes (THP-1) and platelet-monocytes co-culture, after experimental treatment using an ELISA kit according to the manufacturer's instruction (Krishgen Biosystem/ElabBiosciences). Briefly, 100µl of cell culture supernatants/lysates was pipette into each sample well of a 96-well plate as required. After sealing the plate, it was incubated for 90 min at 37˚C. Following the sample's disposal, diluted wash buffer was used four times to wash the plate's well. The plate's wells were then pipetted with diluted biotinylated antibody, and the mixture was incubated for 60 min at 37°C. The plate was again washed four more times, and conjugated HRP was pipetted to each. Subsequently, the plate was incubated for 30 min at 37°C. After final wash, TMB substrate was added to the wells and the plate was incubated for 10 min at 37°C.And, with the use of stop solution, the reaction was stopped and the absorbance (OD) was taken at 450ηm in a multimode microplate reader (Synergy HTX Multi-Mode Reader) within 10-15 min. The levels of protein were estimated from the standard curve.

**Knockdown of HIF-1α, NLRP3, EGR-1 using siRNAs**

In order to perform RNA interference (RNAi), THP-1 cells were maintained to 50–60% confluence in 6 well plates at a cell density of $0.5*10^6$/well. As per the manufacturer's instructions, the cells were transfected using Lipofectamine™ 3000 (Invitrogen, Carlsbad, CA, USA). Briefly, 242.5µl of Opti-

MEM (Invitrogen) was mixed with 1.5µl siRNA of HIF-1α, NLRP3, and EGR-1 gene solution (100µmol) separately and 6µl Lipofectamine$^{TM}$ 3000 and was prepared for each well that was going to be transfected. A gentle mix was made of the two solutions, and they were incubated at RT for 5 min. The solution was added to serum free media and subsequently added to each well. After 8 hrs of incubation in transfection media, the cells were further maintained for an additional 12 hours in fresh complete growth media lacking PS antibiotic at 37°C at 5% CO2.[5]

**Chromatin Immunoprecipitation Assay**

Following the experimental treatment, the cells were fixed in 1% paraformaldehyde, and a Fisher Scientific F550 microtip cell sonicator was used to shear the chromatin that was extracted from the separated nuclei. After centrifugation, the chromatin-sheared supernatants were incubated with either control IgG (Thermo Fisher) or an anti-HIF-1α antibody from Affinity Biosciences. After adding Protein G Sepharose beads and incubating for overnight at 40°C, the immune complexes were eluted. After being subjected to RNase and proteinase K treatment, complexes were extracted using phenol-chloroform method and subsequently use of isopropanol. After precipitating, cleaning, drying, and resuspending in water, DNA was examined using PCR. The primers employed in this analysis, sense (5′-ATTTGGAGTGGCCCGATATGG -3′) and antisense (5′-AGGAAGCCCTAATATGGCAGG -3′), spanned 271bp around the putative HIF-1-binding region within the Egr-1 promoter.

**Microparticles bound tissue factor activity (modified plasma recalcification assay)**

**Preparation and storage of microparticles**

The THP-1 human monocytic cell lines were seeded in six-well plates and differentiated to macrophages with 20 nM PMA for 12 h and kept for 12 h in fresh RPMI-1640 media. After PBS wash, the cells were treated with hypoxia for 8h, DMOG-1000µM for 12 h, DIM-10µM, MCC950-10µM, and SML0499- 10µM for 4 h each. The total microparticles (MPs) were isolated from culture media/cell supernatants immediately after stimulating the cells and pelleting out. Microparticles were sedimented at $2*10^4*g$ at 4°C for 30 min and resuspended at tris-buffered saline (TBS containing- 100M NaCl, 50mM tris-HCl, pH 7.4) containing 1% BSA (TBS/BSA). Immediately after isolation, 0.5 ml aliquots of MPs were frozen in liquid nitrogen in 1.5 ml

eppendorf and stored at -80$^0$ C for not more than a month, but it was preferred to use it immediately.[6]

**Platelet-rich plasma/platelet-poor plasma isolation**

The whole blood of 3-4 healthy individuals was used to isolate plasma. The whole blood of an individual was collected using sodium citrated tube in a proportion of 1:9. The whole blood were mixed and centrifuged at 350*g for 20 min for the production of platelet-rich plasma (PRP) where the supernatant was collected and again centrifuged for 15 min at 2000*g for finally production of platelet-poor plasma (PPP).

**Microparticles bound tissue factor activity (TFU)**

After the isolation of microparticles, it was subjected to tissue factor activity. Platelet-poor plasma (PPP) was stored at 37°C of which 100µl was added in a glass tube containing 100µl cell suspension/thawed MPs which was incubated at 37°C for atleast 2-5 min. In this100µl of 25mM $CaCl_2$ was added and the time for the clot formation was measured by slowly swirling the tube. A standard curve was made using rabbit brain thromboplastin (Sigma) which was suspended saline solution. A serial dilution of thromboplastin was prepared which was added to 100µl of 25 mM $CaCl_2$ and 100µl PPP. By comparing the data to a standard curve, the procoagulant activity is given in arbitrary units (AU) of the results.[6,7]

***In vitro* Platelet Aggregation assay**

K-562 cells were differentiated to platelets with 20 nM PMA and treated with 1000µM DMOG, 10µM DIM, 10µM MCC950, and 10µM SML0499. 100µl ($2\times10^4$) differentiated K-562 cell suspension was added to a pre-prepared 96-well immuno-plate with agonist ADP-10µM. The absorbance and the kinetics of the aggregation for 10 min were recorded on a multimode plate reader (Synergy HTX., Multimode reader) at 575 nm, 600 nm, and 650 nm. The reading was extrapolated with the standard curve obtained from PPP and PRP based on light transmission aggregometry.[8] The % aggregation can be extrapolated against PRP showing 0% aggregation and the transmission of light through PPP as being 100%, hence maximum.

### *In vitro* Platelet Adhesion assay

After experimental treatment to the monocytes and endothelial cells, $0.3*10^6$ differentiated platelets were added to each well of the 12-well plates pre-coated with 10µM collagen solution. The cells were stained with calcein dye at 10µM for 60 min.[9] The cells were kept for 60 min at 37°C to adhere to the coated plates in a $CO_2$ incubator. The loosely attached or non-adherent cells were removed followed by a gentle wash with PBS. After 60 min of incubation in the dark, calcein absorbance was recorded on a multimode plate reader (Synergy HTX, Multimode reader).[10] A standard plot between absorbance and stained cell count (from $0.5 \times 10^4$ to $1 \times 10^6$ cell numbers) was performed before adhesion assays were started. After staining for 60 min with calcein andmild washing, three times with PBS, stained cells were suspended at a series of concentrations to determine their fluorescence intensity.[3,4]

### Calcium Mobilization

The effect of hypoxia-mediated calcium mobilization was studied according to Ishii et al. with slight modifications.[52] Briefly, 2µM Fluo-4 AM was incubated with a differentiated megakaryocytic cell line for 1 hour at 37℃. The cells were collected by centrifuging for 5 min at 1500*g. Subsequently the cell pellet at cell density of $5x10^6$ cells/ml in serum-free media. For extracellular calcium, 1 mM $CaC1_2$ was added prior to incubation for 5 min at 37℃. Later the cells were stimulated with thrombin, and the fluorescent intensity was recorded at an excitation and emission of 485/20ηm and 528/20ηm wavelengths respectively using Synergy HTX Multimode Microplate Reader (BioTek). To obtain the fluorescence signals at maximal $Ca^{2+}$ saturation of the dye. Further, the platelets were lysed by the addition of 0.1% Triton X-100 and 8mM EGTA added to obtain the maximum and minimum fluorescent signals respectively. The $Ca^{2+}$ levels were calculated as previously described by Gee KR.[11]

### Animal Sample collection and storage

The thrombus was separated from IVC and was measured for length and weight after that it was immediately snap-frozen and stored for further experiments. The blood samples were collected by retro-orbital vein in 3.2% trisodium citrate in a volume ratio of 9:1. The sample tubes were centrifuged at 2000*g for 20 min at RT to separate and collect plasma. Fresh plasma was used for

activated partial thromboplastin time (aPTT), prothrombin time (PT), platelet adhesion, and aggregation whereas the rest was deep-frozen (–80°C) for future investigation.

**$FeCl_3$ induced thrombosis model**

To model the thrombosis, $FeCl_3$ tissue injury model was used.[12] Animals were given free access to food and water before surgery. Intraperitoneal injections of ketamine and xylazine (ketamine 50mg/kg and xylazine 10 mg/kg) were used to anesthetize rats. While performing median laparotomy the animals were placed in a supine position. The abdominal organs were exteriorized and placed on sterile impregnated gauze to prevent drying. For the $FeCl_3$-induced model, the inferior vena cava (IVC) having fat deposits was carefully cleaned and filter paper (1mm×1mm×1mm) with 10% $FeCl_3$ was placed superficially on the top of the IVC. After 4 min of induction, the filter paper was removed and the abdominal organs were placed back carefully in the abdomen and sterile saline was applied during the entire procedure to prevent drying of organs. The peritoneum and skin were closed with interrupted suture. The rats were kept back in cages without having husks. Only one rat was kept per cage to avoid disturbance by the other. Rats were euthanized after the designated time point and gross thrombus was inspected *in situ.* The thrombus is harvested by excising IVC from the confluence of the iliac veins. The attached muscular tissue, artery, and ligatures were removed by microdissection to have only an IVC-containing thrombus.

**Thrombus weight, length determination**

The measurement of thrombus size and weight provides an indirect way of accessing thrombus formation and resolution. The harvested IVC having thrombus was split longitudinally, and the thrombus was removed. According to the previously reported method by Myers et al., 2002, the thrombus was weighed (mg) and length was measured (mm).[13]

**NO concentration in plasma**

The Griess reagent (Sigma-Aldrich) technique was used to detect the amount of nitric oxide (NO) in plasma. This technique detects nitrite (NO2-), one of the two main, stable, and nonvolatile breakdown products of NO. It is based on a chemical phenomenon that use sulfanilamide and N-1-naphthyl ethylenediamine dihydrochloride in the presence of phosphoric acid (acidic

environment), the Griess Reagent System is a method for analyzing chemical reactions. Following the manufacturer's recommendations, a 96-well microliter plate was used to measure the NO concentration. After 10 min, the absorbance was recorded in OD using a multimode plate reader at a wavelength 540 ηm. The samples, standards, and controls were all measured and expressed in μM.

**eNOS activity**

In platelets, eNOS enzyme activity was quantified using a fluorometric detection system (BioTek, USA) and expressed in Units of Fluorescence (UF) per min (m) /1*$10^6$ platelet cells.[9,14] Triazolofluoresceine, which is produced from 4, 5-diaminofluoresceine diacetate by intracellular esterase, is known to fluoresces when NO interacts with it. The wavelengths for excitation and emission were 485ηm and 515ηm, respectively. Since endothelial NOS is only activated in platelets, the activity of this specific isoform was only measured and expressed as UF/mn.

**Platelets adhesion**

Platelets from all the treated animals were isolated which was fluorescently labeled and allowed to adhere to collagen (10uM) coated wells for up to 60 min at 37°C. Quantification of platelet adhesion was done with the fluorescence intensity at 485/20, and 528/20 on a multimode plate reader (Synergy HTX., Multimode reader). The result was extrapolated with the standard curve with a known number of platelets.

**Platelets aggregation**

For platelets aggregation, PRP was separated from the whole blood of all the treated groups, incubated for 5 min at 37°C. It was induced with agonist like Adenosine diphosphate (ADP). The rate and the extent of ADP-induced platelet aggregation were recorded with rotational shaking initially.

**aPTT, PT**

A semi-automated coagulation analyzer (Labitec) was used to do aPTT and PT assays as per the manufacturer’s instructions. For conducting aPTT assay 50µl plasma was incubated with 50µl of

aPTT reagent (C.K. PREST® 5, Stago) in a cuvette for 3 min placed at 37°C, followed by recalcification with 50µl of 25 mM $CaCl_2$ clotting time was recorded in sec.

For PT assay, 50µl of plasma was pipetted in a cuvette and incubated for 2 min at 37°C. Later 100µl PT reagent was added to it (NÉOPLASTINE® CI PLUS, STAGO), a recombinant tissue factor. The clotting time was recorded in sec.

**Tail-bleeding assay**

The tail bleeding assay was done by giving anaesthesia to the animal and transacting the tail 0.5 cm from the tail tip using a fresh disposable surgical blade. Immediately after being cut tail was vertically placed in 10 ml isotonic saline at RT and bleeding time was recorded until the bleeding had ceased completely.

**Results**

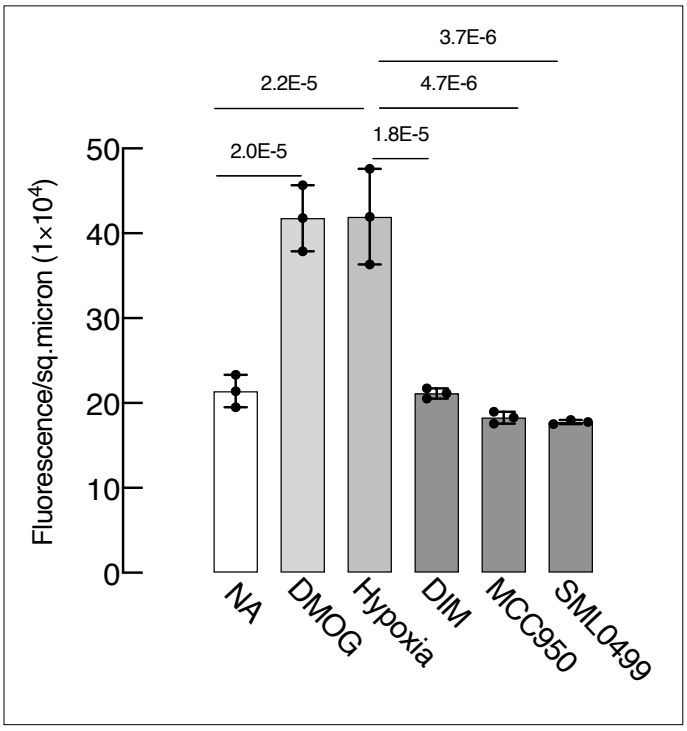


**Figure S1: Adherence of monocytes to endothelial cells.** HUVECs were exposed to hypoxia for 8h for all experimental conditions. Purified monocytes (hPBMCs) isolated from whole blood and treated to various experimental conditions and added to ECs for 20min to adhere to it. Statistical

analysis was performed using the One-way ANOVA with the Tukey multiple comparison test. Data is represented as SEM ±.

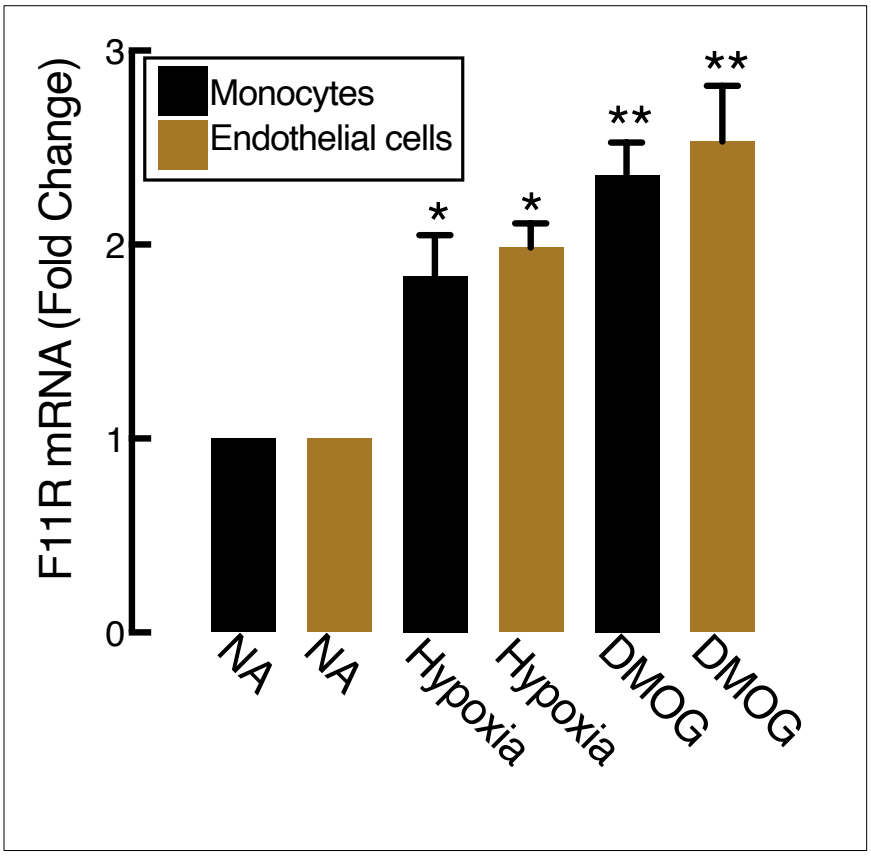


**Figure S2: Regulation of F11R transcripts.** The F11R gene is expressed by monocytes and endothelial cells including others. To overrule its expression in the different cells, we determine the interaction of monocytes with endothelial cells. F11R expression was quantified independently in different cells under hypoxia and DMOG. Statistical analysis was performed using the One-way ANOVA with the Turkey multiple comparison test. Data is represented as SEM ±.

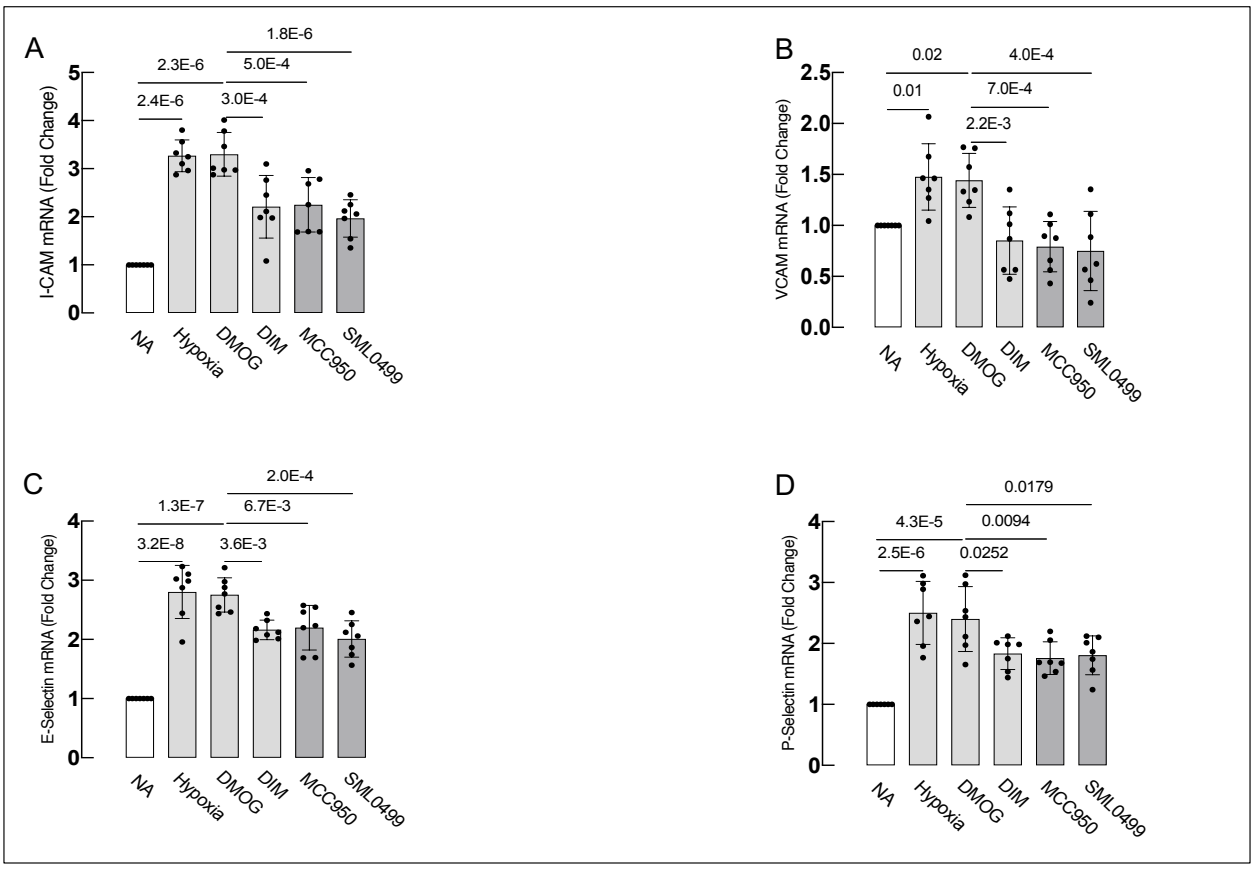


**Figure S3: Recruitment of endothelial adhesion molecules leads to endothelial dysfunction.** Endothelial cells were treated with hypoxia (1% $O_2$) for 8 h, HIF-1α activator, Dimethyloxalylglycine (DMOG) for 12 h, DMOG+HIF-1α inhibitor-DIM, NLRP3 inhibitor-MCC950+DMOG and the inhibitor of catalytic activity of caspase-1-SML0499+DMOG. All the inhibitors were used for 4 h each: **A,** RNA expression of I-CAM; **B,** VCAM; **C,** E-Selectin; **D,** P-selectin. Statistical analysis was performed using the One-way ANOVA with the Tukey multiple comparison test. Data is represented as SEM ±.

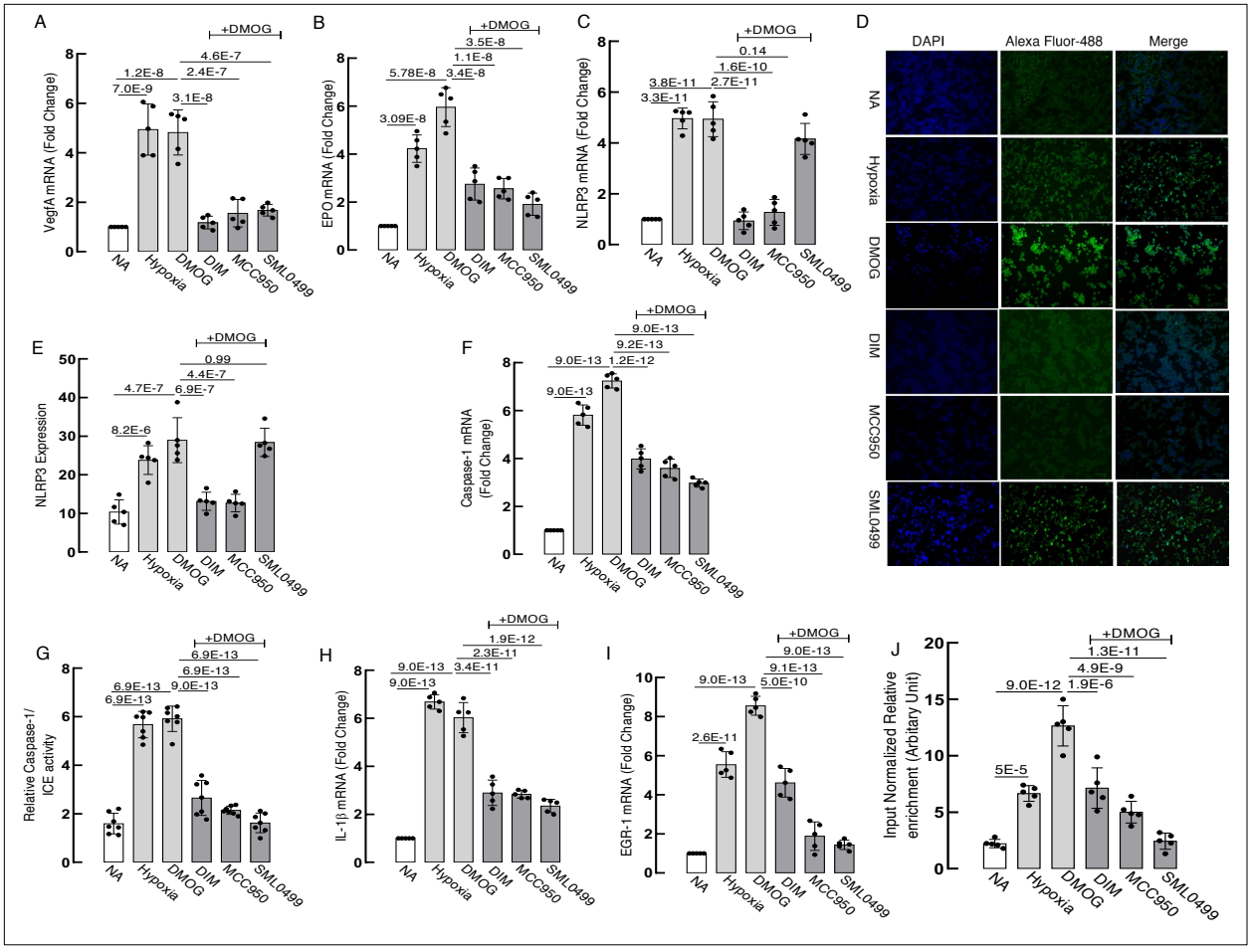


**Figure S4: Implication of hypoxia in regulation of NLRP3 inflammasome axis.** Monocytes were treated with experimental conditions. We determined mRNA expression of **A**, VEGF-A; **B,** EPO. Hypoxia exposure results in a pro-inflammatory state. **C,** NLPR3 mRNA transcripts, **D,** Representation of NLRP3 immunocytochemistry staining with Alexa Fluor 488; **E,** Relative NLRP3 fluorescence signal revealed hypoxia and DMOG induced NLRP3 protein; **F,** Caspase-1 mRNA transcript; **G,** Relative Caspase-1/Interleukin-1 (IL-1) converting enzyme (ICE) activity; and **H,** Protein expression of cytokine IL-1β; **I,** Relative mRNA expression of Egr-1 under different experimental conditions; The expression of the gene was normalized with 18sRNA, as an internal control to that of the NA group; J, The enrichment of the Egr-1 promoter region in CHIP experiments was quantified and the bar graph was plotted. Statistical analysis was performed using the One-way ANOVA with the Tukey multiple comparison test. Data is represented as SEM ±.

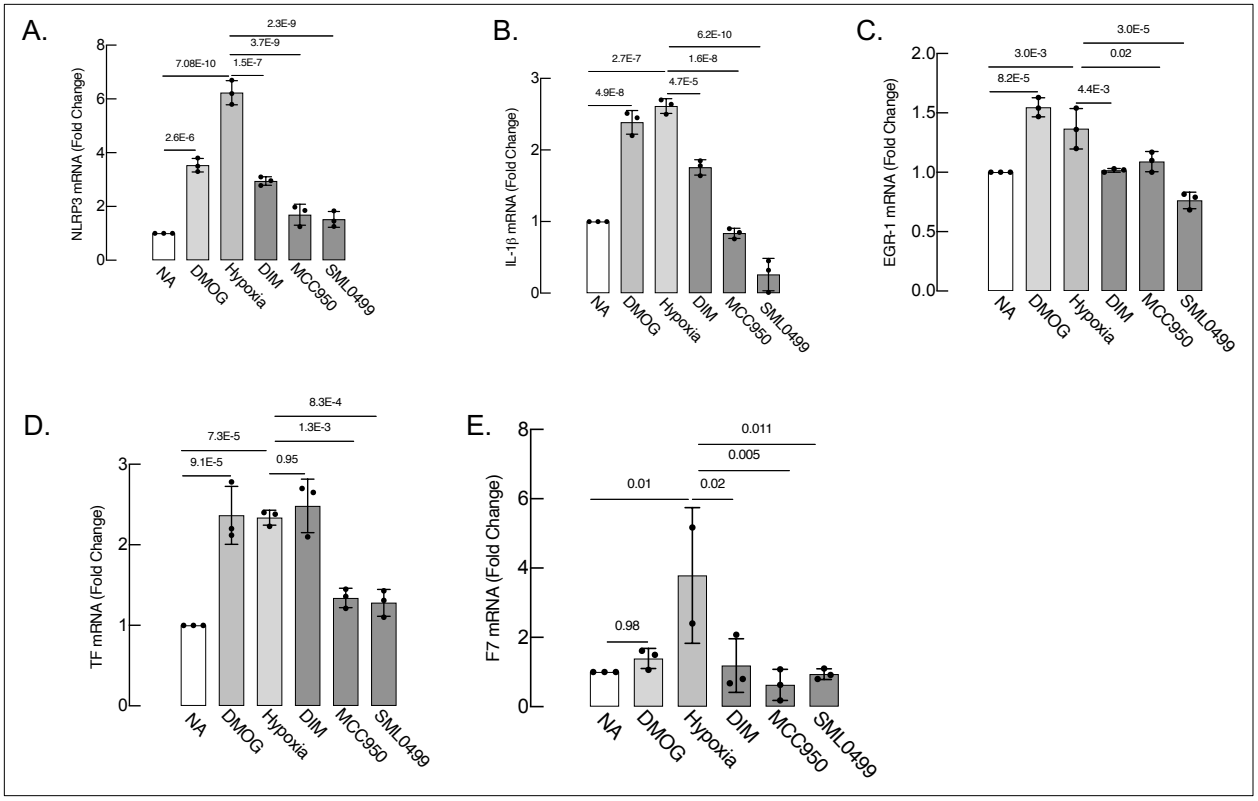


**Figure S4A: Hypoxia exposure results in a pro-inflammatory and prothrombotic state.** hPBMCs were treated to all the experimental conditions. RNA was isolated and mRNA expression was analyzed. A. NLRP3; B. IL-1β; C. Egr-1; D. Tissue factor; E. F7 expression under different experimental conditions. The expression of the gene was normalized with 18sRNA, as an internal control to that of the NA group. Statistical analysis was performed using the One-way ANOVA with the Tukey multiple comparison test. Data is represented as SEM ±.

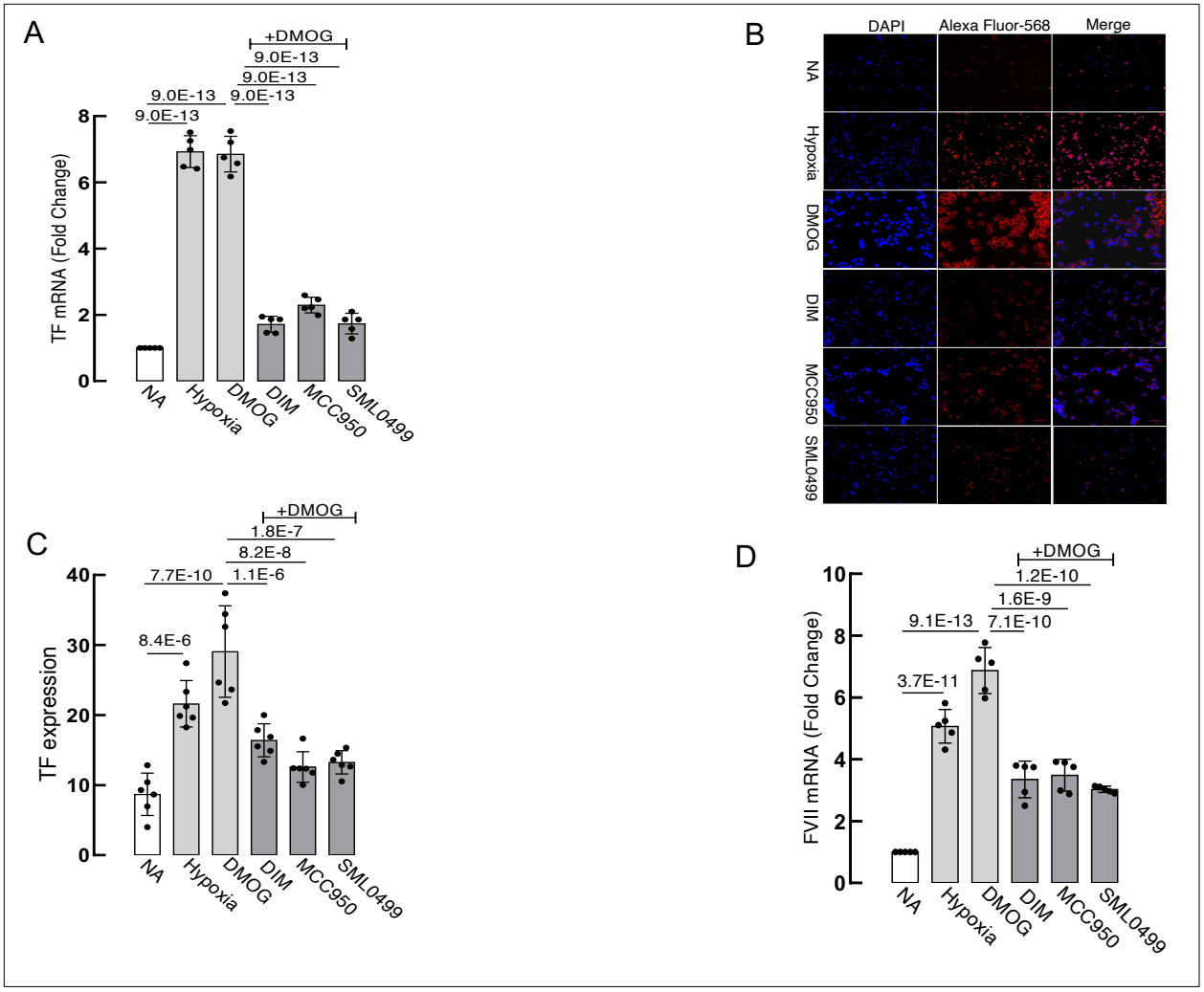


**Figure S5: Hypoxia induced prothrombotic state.** Expression of tissue factor (TF), a initiator of coagulation. **A,** Relative mRNA expression of TF; **B,** Represenation of TF immunocytochemistry staining with Alexa Fluor 568; **C,** Relative fluorescence signal revealed hypoxia and DMOG induced TF protein levels while its suppressed by inhibiting HIF-1α, NLRP3 and catalytic activity of caspase-1. **D,** Relative mRNA levels of FVII transcripts in all experimental conditions. Statistical analysis was performed using the One-way ANOVA with the Tukey multiple comparison test. Data is represented as SEM ±.

**Correlation**

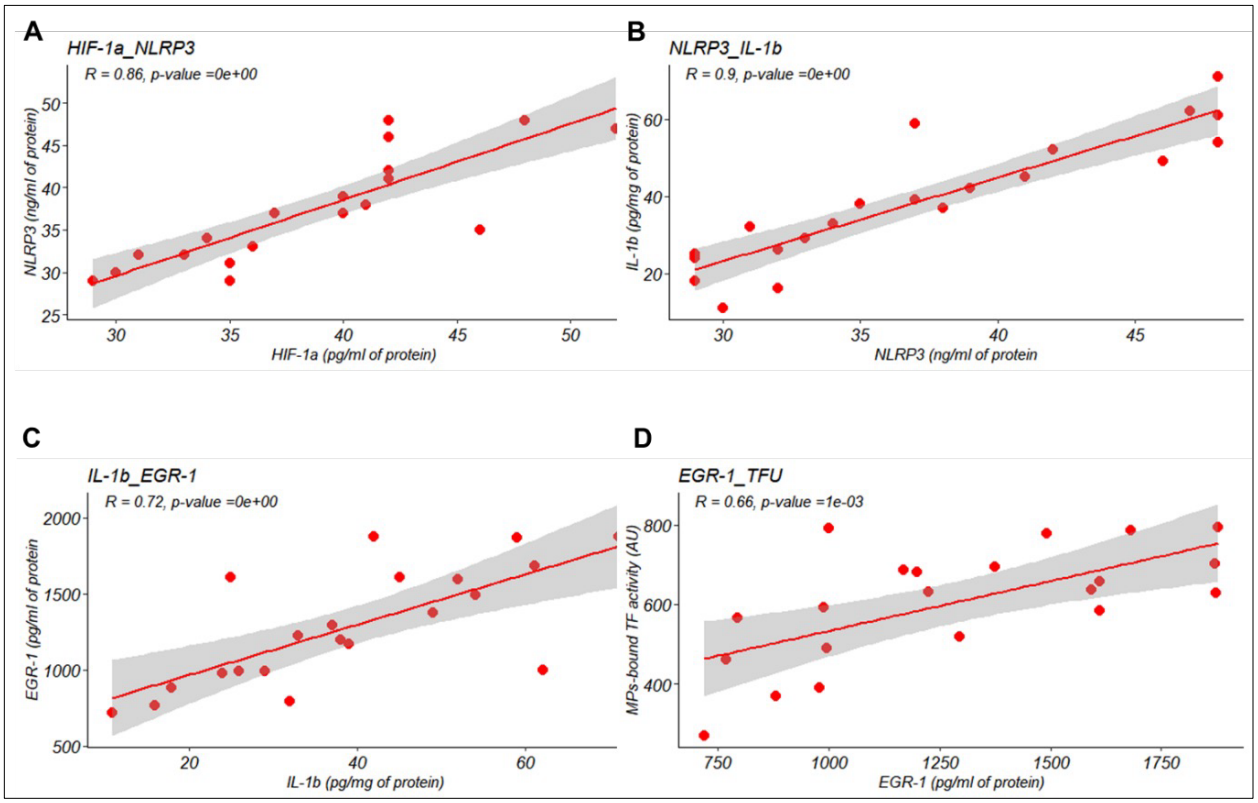


**Figure S6: Egr-1 protein contributed to the hypoxia-induced tissue factor activity (Tfu**). **A,** The protein concentration of HIF-1α (pg/ml) was significantly correlated with the concentrations of NLRP3 (ng/ml). **B,** The protein concentration of NLRP3 (ng/ml) was significantly correlated with the concentrations of IL-1 β (pg/ml). **C,** The protein concentration of IL-1β (pg/ml) was significantly correlated with the concentrations of Egr-1 (pg/ml). **D,** The protein expression of Egr-1 (pg/ml) was significantly correlated with MPs-bound tissue factor activity (TFU/AU). Pearson Correlation analysis was used for correlation analysis as data met the criteria of normal distribution and collinearity.

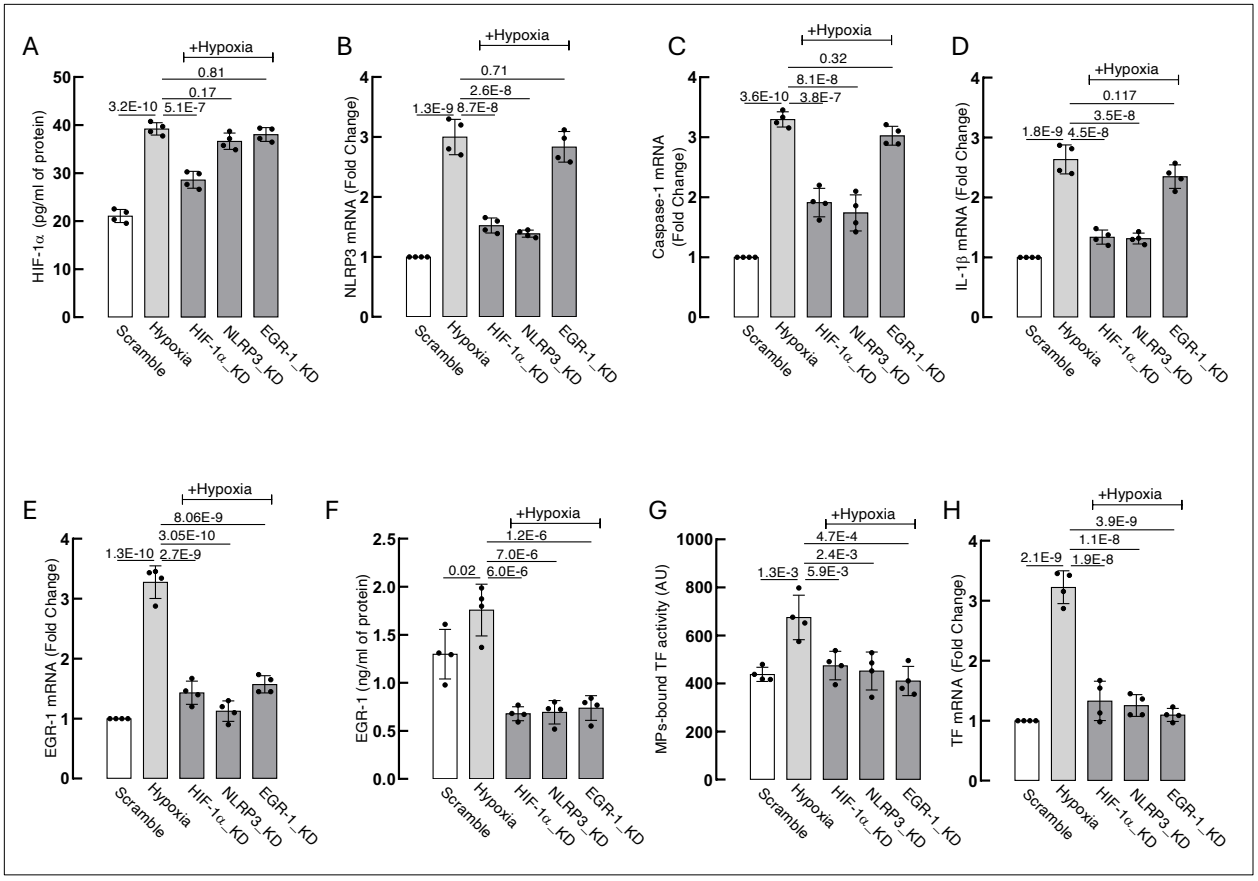


**Figure S7: Egr-1 promotes thrombogenesis through tissue factor expression via HIF-1a-NLRP3 inflammasome axis:** THP-1 cells were cultured and treated with siRNA of HIF-1α, NLRP3 and Egr-1 for 6 hrs and then exposure to hypoxia; **A,** Protein levels of HIF-1α under different experimental conditions; **B,** Relative levels of NLRP3; **C,** Caspase-1; **D,** IL-1β; **E,** Egr-1 transcripts, and **F,** Egr-1 protein level; **G,** Estimation of microparticles bound tissue factor activity, and **H,** Relative expression of F3 in all the experimental conditions. (Comparison was done Scramble v/s Hypoxia; Hypoxia versus HIF-1α, NLRP3, and EGR-1 knockdown). 18sRNA was used as an internal control and expression was normalized to that of Scramble; Statistical analysis was performed using the One way ANOVA with the Tukey multiple comparison test. Data is represented as SEM ±.

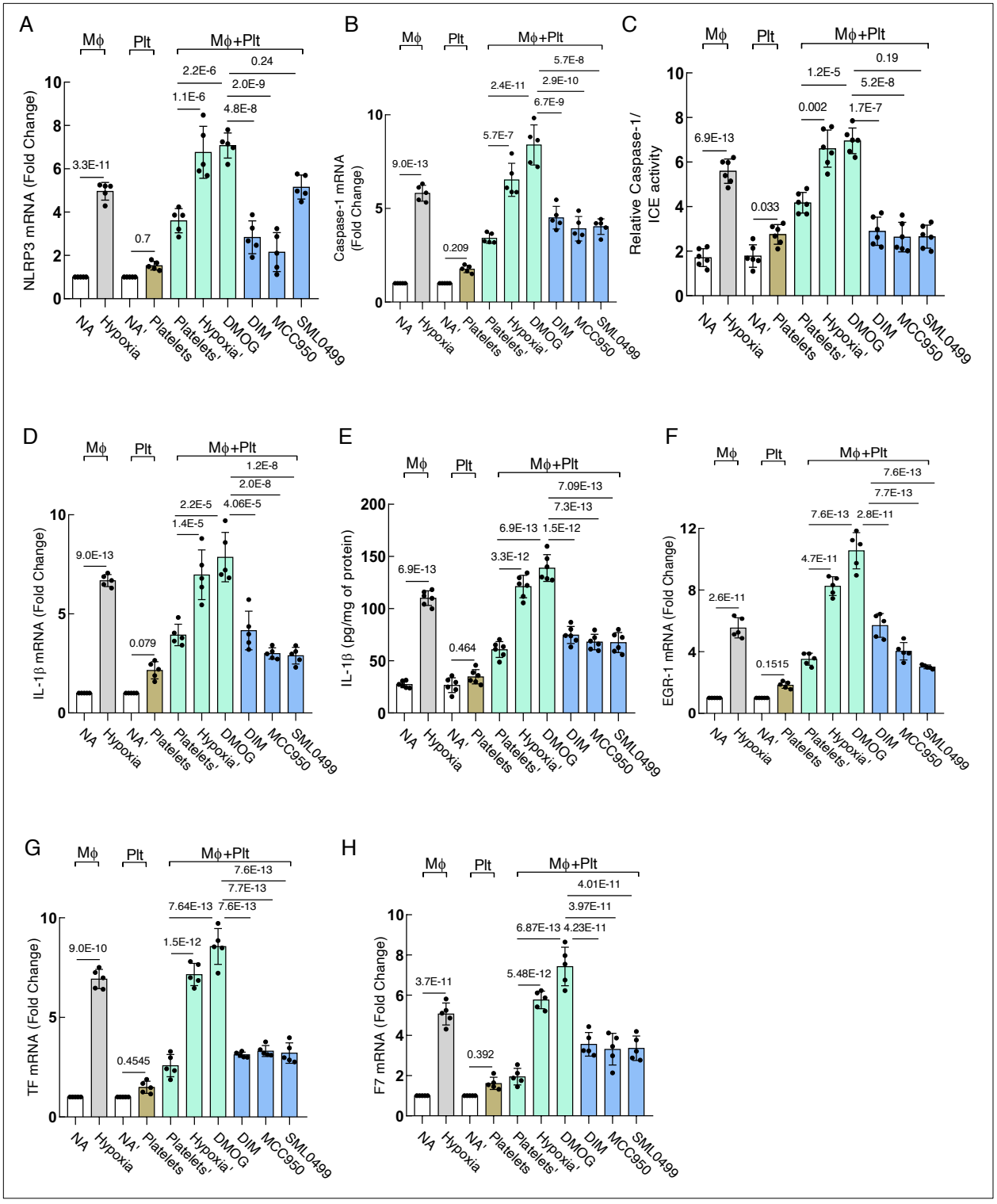


**Figure S8**: Platelets strengthen the pro-inflammatory and pro-thrombotic milieu under hypoxia. **A,** Relative expression of NLRP3 transcripts; **B-C**, Caspase-1 transcript and Caspase-1/Interleukin-1 (IL)-1 converting enzyme (ICE) activity respectively; **D-E,** IL-1β transcripts and

protein levels of Cytokine IL-1β; **F,** Egr1 mRNA transcripts; **G-H,** mRNA transcripts of Tissue factor and Factor 7 in all the experimental conditions. The expression of the gene was normalized with 18sRNA, as an internal control to that of the NA group. Statistical analysis was performed using the One-way ANOVA with the Tukey multiple comparison test. Data is represented as SEM ±.

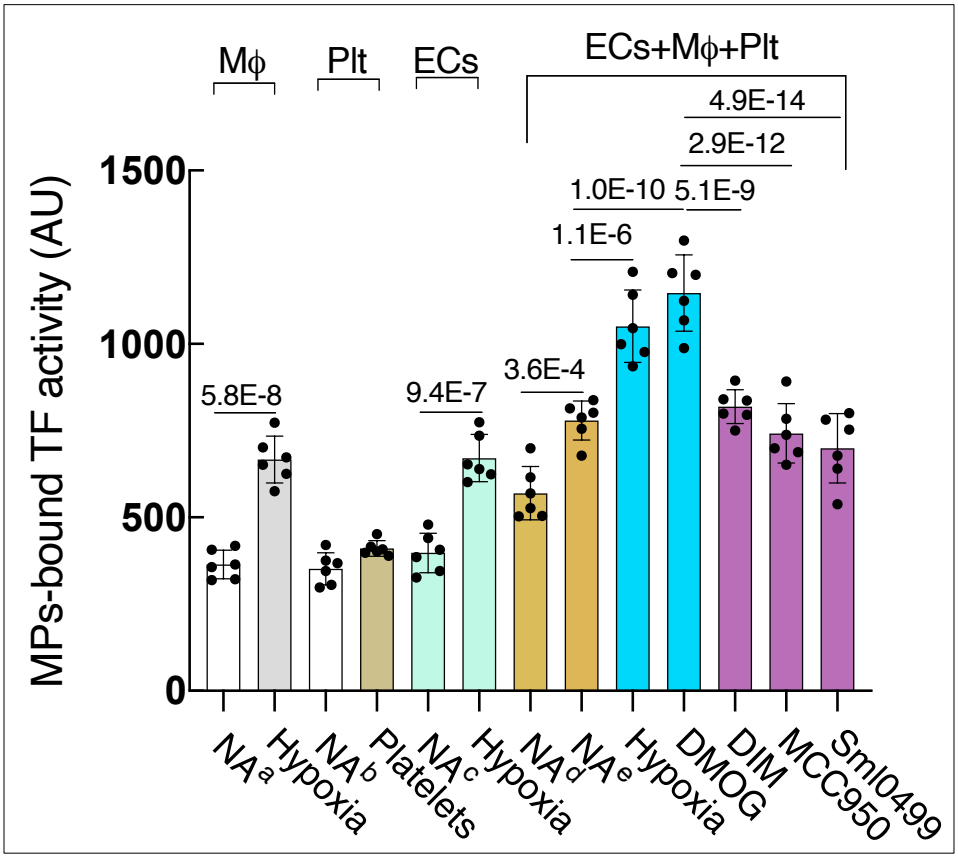


**Figure S9: Platelets strengthen pro-thrombotic milieu under hypoxia.** Endothelial cells (ECs) were pre-treated with 1% $O_2$ (hypoxia) for 8h for all the experimental condition of monocytes; Monocytes were treated with hypoxia, DMOG, DIM, MCC950, and SML0499. Platelets were pre-activated with ADP and washed before adding to co-culture of ECs and Monocytes. **A.** Microparticles bound tissue factor activity in different experimental conditions. No addition ($NA^a$) of monocytes; No addition ($NA^b$) of platelets; $NA^c$ of ECs; $NA^d$ of ECs, monocytes and Platelets; $NA^e$ of monocytes, Platelets and activated ECs. Statistical analysis was performed using the One-way ANOVA with the Tukey multiple comparison test. Data is represented as SEM ±.

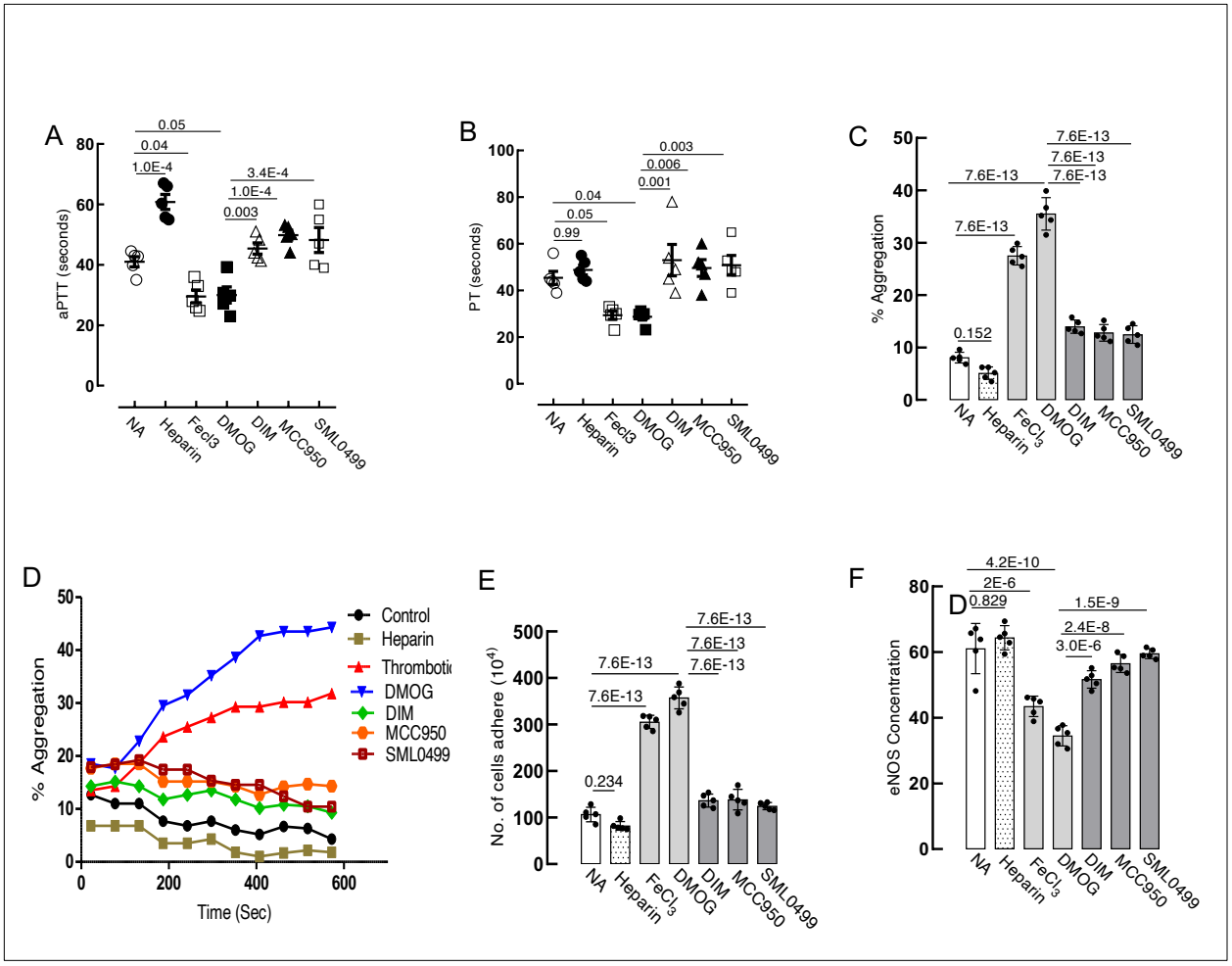


**Figure S10: Acceleration of venous thromboembolism through HIF-1α-NLRP3-Egr-1 axis.** **A,** aPTT (Activated Partial Thromboplastin Time); **B,** PT (Prothrombin Time); **C,** Platelets percent aggregation under the influence of hypoxia through HIF-1a-NLRP3; **D,** Kinetics of platelets aggregation at different time point; **E,** Platelets adhesion to collagen; **F,** eNOS concentration under all the experimental condition in-vivo. Statistical analysis was performed using the One-way ANOVA with the Tukey multiple comparison test. Data is represented as SEM ±.

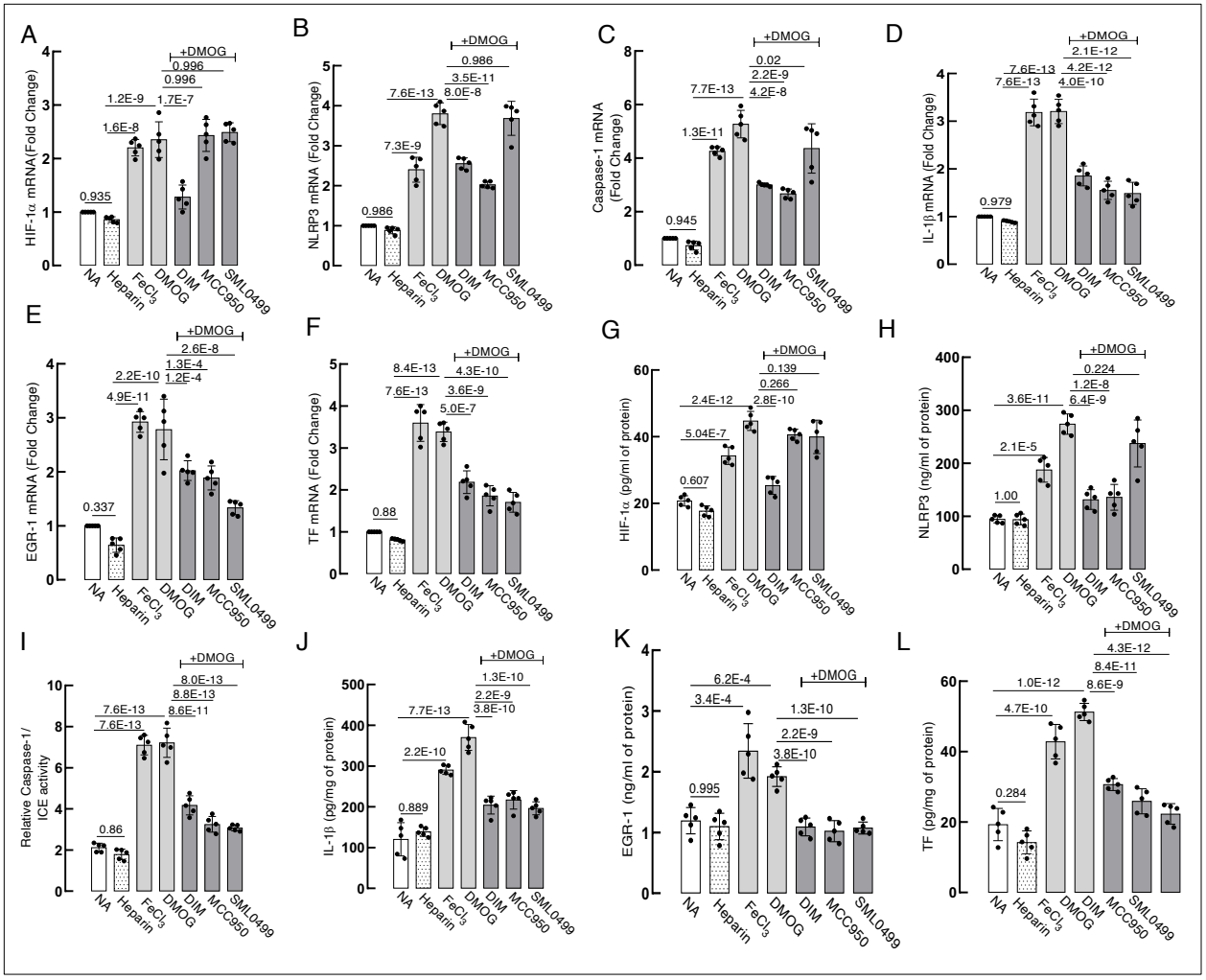


**Figure S11. Hypoxia induced pro-inflammatory and pro-thrombotic state through HIF-1a-NLRP3-Egr-1 axis.** A-F, Relative levels of **A**, HIF-1α; **B**, NLRP3; **C**, Caspase-1; **D**, IL-1β; **E**, Egr-1, and **F**, F3 transcripts in all experimental condition as described; G-L, Estimation of protein level of **G**, HIF-1α; **H**, NLRP3, **I**, Caspase-1/Interleukin converting enzyme-1 activity; **J**, IL-1β, **K**, Egr-1, and **L**, F3 by ELISA in all the experimental conditions. β-actin was used as an internal control and expression was normalized to that of NA group; Statistical analysis was performed using the One way ANOVA with the Tukey multiple comparison test. Data is represented as SEM ±.

Table S1: Demographic, and clinical, characteristics of patients with DVT

| Characteristics | | Patients (n=10) | Healthy (n=10) | P-value |
|---|---|---|---|---|
| Age, years Median (Range) | | 46 (27-65) | 42 (27-60) | 0.2303 |
| BMI | | 24.52 | 22.93 | 0.2644 |
| Gender (F/M) | | 3/7 | 4/6 | - |
| Food habit (Veg/Both) | | 2/8 | 3/7 | - |
| BP | SBP, mmHg | 96-118 | 120 | 0.0051 |
| | DBP, mmHg | 60-95 | 80 | 0.0835 |
| PR, rate/min | | 88-95 | 56-100 | 0.0698 |

F, Female; M, Male; BMI, Body mass index; n, number of subjects; SBP, systolic blood pressure; DBP, diastolic blood pressure; PR-Pulse Rate

Table S2: List of gene with its Real-time PCR primer sequence.

| **Oligonucleotides** | | |
|---|---|---|
| Gene symbol | Sequence | Company |
| CD18 | 5'-CTGGTAGCAAAGCCCCCACG-3' (Sense) and 5'-TGGGTTTCAGCGAGGCTTGTG-3' | Sigma-Aldrich |
| F11R | 5'-CTGTCCTGGTAACACTGATTCTC-3'(Sense) and 5'-TCTGTTTGAATTCTCCCTCACTG-3' (antisense) | Sigma-Aldrich |
| HIF-1α | 5'-GCTACTACATCACTTTCTTGG-3' (Sense) and 5'-TCTACATGCTAAATCAGAGGG-3' (antisense) | Sigma-Aldrich |
| NLRP3 | 5'-CATTGAGAACTGTCATCGGG-3' (sense) and 5'-GCTGTTCACCAATCCATGAG-3'(antisense) | Sigma-Aldrich |
| Casp-1 | 5'-ATGTTGAATACCAAGAACTGCC-3' (sense) and 5'-CCAAGAAACATTATCTGGTGTGG-3' (antisense) | Sigma-Aldrich |
| IL-1β | 5'-ACAGATGAAGTGCTCCTTCC-3' (sense) and | Sigma-Aldrich |

| | | |
|---|---|---|
| | 5’-CACATAAGCCTCGTTATCCCA-3’ (antisense) | |
| V-CAM | 5’-GCAAGTCTACATATCACCCA-3’ (sense) and<br>5’-AATCTTCCATCCTCATAGCA-3’ (antisense) | Sigma-Aldrich |
| E-selectin | 5’-CTGCCTGTACCAATACATCC-3’ (sense) and<br>5’-CAGTTCACAATTTGCTCACAC-3’ (antisense) | Sigma-Aldrich |
| P-selectin | 5’-CAGAGTCACAGAGGAGATGG-3’ (sense) and<br>5’-TTTGTTAGTTCAGAGATCAGGG-3’ (antisense) | Sigma-Aldrich |
| VEGF-A | 5’-CTCCGAAACCATGAACTTTCTG-3’ (sense) and<br>5’-CATGAACTTCACCACTTCGT-3’ (antisense) | Sigma-Aldrich |
| EPO | 5’-GCATGTGGATAAAGCCGTCAGTG-3’ (sense) and<br>5’-GAGTTTGCGGAAAGTGTCAGCAG-3’ (antisense) | Sigma-Aldrich |
| TF | 5’-CAAATAAGCACTAAGTCAGGAG-3’ (sense) and<br>5’-ATCTTCTACGGTCACATTCAC-3’ (antisense) | Sigma-Aldrich |
| FVII | 5’-CACACCCACAGTTGAATATCC-3’ (sense) and<br>5’-GCTCCATTCACCAACAACAG-3’ (antisense) | Sigma-Aldrich |
| uPA | 5’-CACTGCTTCATTGATTACCCA-3’ (sense) and<br>5’-TTTCCACCTCAAACTTCATCTC-3’ (antisense) | Sigma-Aldrich |
| tPA | 5’-AGAGGAGCCAGATCTTACCA-3’ (sense) and<br>5’-TGGCCCTGGTATCTATTTCAC-3’ (antisense) | Sigma-Aldrich |
| PAI-1 | 5’-GAACTTCAGGATGCAGATGTC-3’ (sense) and<br>5’-CCCTTGTCATCAATCTTGAATCC-3’ (antisense) | Sigma-Aldrich |
| EGR-1 | 5’-ATTTGGAGTGGCCCGATATGG-3’ (sense) and<br>5’-AGCAGGAAGCCCTAATATGGC-3’ (antisense) | Sigma-Aldrich |
| 18sRNA | 5’-CTTAGAGGGACAAGTGGCG -3’ (sense) and<br>5’-ACGCTGAGCCAGTCAGTGTA -3’ (antisense) | Sigma-Aldrich |
| **Rat** | | |
| HIF-1α | 5’-CACCTTCTACCCAAGTACCT-3’ (sense) and<br>5’-GTAACGTTCCAATTCCTGCT-3’ (antisense) | Sigma-Aldrich |
| NLRP3 | 5’- ACATTCAGAGACTGTGGTTGG-3’ (sense) and<br>5’- ATGCGAGATCCTGACAACAC-3’ (antisense) | Sigma-Aldrich |

| | | |
|---|---|---|
| Caspase-1 | 5’- GCTTCAGTCAGGTCCATCAG-3’ (sense) and<br>5’- TTCTTTCCATAACTTCTGGGCT-3’ (antisense) | Sigma-Aldrich |
| IL-1β | 5’- CAAATCTCACAGCAGCATCTC-3’ (sense) and<br>5’- GTCATCATCCCACGAGTCAC-3’ (antisense) | Sigma-Aldrich |
| Egr-1 | 5’- CAAACTGGAGGAGATGATGCTG-3’ (sense) and<br>5’- AAAGGACTCTGTGGTCAGGT-3’ (antisense) | Sigma-Aldrich |
| TF | 5’- ACCCACCAACTATACCTACAC-3’ (sense) and<br>5’-TCACATCCTTCACAATCTCGT<br>-3’ (antisense) | Sigma-Aldrich |
| β-actin | 5’- AGATGACCCAGATCATGTTTGAG-3’ (sense) and<br>5’- TTAATGTCACGCACGATTTCC-3’ (antisense) | Sigma-Aldrich |

## References


1. Saito H. (1997). Megakaryocytic cell lines. Bailliere's clinical haematology, 10(1), 47–63. https://doi.org/10.1016/s0950-3536(97)80050-9
2. Langer F, Spath B, Fischer C, Stolz M, Ayuk FA, Kröger N, Bokemeyer C, Ruf W. Rapid activation of monocyte tissue factor by antithymocyte globulin is dependent on complement and protein disulfide isomerase. Blood. 2013 Mar 21;121(12):2324-35. doi: 10.1182/blood-2012-10-460493.
3. Yasmin R, Chanchal S, Ashraf MZ, Doley R. Daboxin P, a phospholipase $A_2$ of Indian Daboia russelii venom, modulates thrombin-mediated platelet aggregation. J Biochem Mol Toxicol. 2023 Nov;37(11):e23476. doi: 10.1002/jbt.23476. Epub 2023 Jul 19. PMID: 37466159.
4. Kong, T., Eltzschig, H. K., Karhausen, J., Colgan, S. P., & Shelley, C. S. (2004). Leukocyte adhesion during hypoxia is mediated by HIF-1-dependent induction of beta2 integrin gene expression. Proceedings of the National Academy of Sciences of the United States of America, 101(28), 10440–10445. https://doi.org/10.1073/pnas.0401339101
5. Han H. (2018). RNA Interference to Knock Down Gene Expression. Methods in molecular biology (Clifton, N.J.), 1706, 293–302. https://doi.org/10.1007/978-1-4939-7471-9_16
6. Khaspekova, S. G., Antonova, O. A., Shustova, O. N., Yakushkin, V. V., Golubeva, N. V., Titaeva, E. V., Dobrovolsky, A. B., & Mazurov, A. V. (2016). Activity of Tissue Factor in Microparticles Produced in vitro by Endothelial Cells, Monocytes, Granulocytes, and Platelets. Biochemistry. Biokhimiia, 81(2), 114–121. https://doi.org/10.1134/S000629791602005X
7. Di Stefano, R., Barsotti, M. C., Armani, C., Santoni, T., Lorenzet, R., Balbarini, A., & Celi, A. (2009). Human peripheral blood endothelial progenitor cells synthesize and express functionally active tissue factor. Thrombosis research, 123(6), 925–930. https://doi.org/10.1016/j.thromres.2008.10.013
8. Chan, M. V., Armstrong, P. C., & Warner, T. D. (2018). 96-well plate-based aggregometry. Platelets, 29(7), 650–655. https://doi.org/10.1080/09537104.2018.1445838
9. Martins Lima, A., Saint Auguste, D. S., Cuenot, F., Martins Cavaco, A. C., Lachkar, T., Khawand, C. M. E., Fraga-Silva, R. A., & Stergiopulos, N. (2020). Standardization and Validation of Fluorescence-Based Quantitative Assay to Study Human Platelet Adhesion

to Extracellular-Matrix in a 384-Well Plate. International journal of molecular sciences, 21(18), 6539. https://doi.org/10.3390/ijms21186539

10. Tyagi, T., Ahmad, S., Gupta, N., Sahu, A., Ahmad, Y., Nair, V., Chatterjee, T., Bajaj, N., Sengupta, S., Ganju, L., Singh, S. B., & Ashraf, M. Z. (2014). Altered expression of platelet proteins and calpain activity mediate hypoxia-induced prothrombotic phenotype. Blood, 123(8), 1250–1260. https://doi.org/10.1182/blood-2013-05-501924
11. Gee, K. R., Brown, K. A., Chen, W. N., Bishop-Stewart, J., Gray, D., & Johnson, I. (2000). Chemical and physiological characterization of fluo-4 Ca(2+)-indicator dyes. Cell calcium, 27(2), 97–106. https://doi.org/10.1054/ceca.1999.0095
12. Li, W., Nieman, M., & Sen Gupta, A. (2016). Ferric Chloride-induced Murine Thrombosis Models. Journal of visualized experiments: JoVE, (115), 54479. https://doi.org/10.3791/54479
13. Myers, D., Wrobleski, S., Londy, F., Fex, B., Hawley, A., Schaub, R., Greenfield, L., & Wakefield, T. (2002). New and effective treatment of experimentally induced venous thrombosis with anti-inflammatory rPSGL-Ig. Thrombosis and haemostasis, 87(3), 374–382.
14. Dosenko, V. E., Zagoriy, V. Y., Haytovich, N. V., Gordok, O. A., & Moibenko, A. A. (2006). Allelic polymorphism of endothelial NO-synthase gene and its functional manifestations. *Acta biochimica Polonica*, *53*(2), 299–302.